Review

Fractional Analytic QCD: The Recent Results

Anatoly Kotikov *, Ilnur Gabdrakhmanov, Nikita Gramotkov, Oleg Teryaev, Daria Volkova, Ivan Zemlyakov

Posted Date: 16 December 2024

doi: 10.20944/preprints202412.1263.v1

Keywords: fractional analytic; QCD; Bjorken sum rule

Review

Fractional Analytic QCD: The Recent Results

I.R. Gabdrakhmanov [1], N.A Gramotkov [1,2], A.V. Kotikov [1,*], O.V. Teryaev [1], D.A. Volkova [1,3] and I.A. Zemlyakov [4]

[1] Bogoliubov Laboratory of Theoretical Physics, Joint Institute for Nuclear Research, 141980 Dubna, Russia
[2] Moscow State University, 119991, Moscow, Russia
[3] Dubna State University, 141980 Dubna, Moscow Region, Russia
[4] Department of Physics, Universidad Tecnica Federico Santa Maria, Avenida Espana 1680, Valparaiso, Chile
* Correspondence: kotikov@theor.jinr.ru

Abstract: In this work, we present an overview of fractional analytic QCD in the spacelike (Euclidean) and timelike regions, which significantly improves the coupling constant in perturbative QCD. The obtained results are applied to the description of the Higgs boson decay into a bottom-antibottom pair and the polarized Bjorken sum rule. For the latter, an additional modification is proposed to combine the fitting curve with the condition for photoproduction.We found good agreement between the experimental data obtained for the polarized Bjorken sum rule and the predictions of analytic QCD, as well as a strong difference between these data and the results obtained in the framework of perturbative QCD. To satisfy the limit of photoproduction and take into account Gerasimov-Drell-Hearn and Burkhardt-Cottingham sum rules, we develope new representation of the perturbative part of the polarized Bjorken sum rule. We present an overview of fractional analytic QCD and its application for Higgs-boson decay into a bottom-antibottom pair and the description of the polarized Bjorken sum rule. The results shown here have been recently obtained in Refs. [18,19,21,22]. This study is dedicated to the description of the polarized Bjorken sum rule, based on recently derived formulas within the analytic QCD approach. To accommodate the photoproduction limit and incorporate the Gerasimov-Drell-Hearn and Burkhardt-Cottingham sum rules, we develop a new representation for the twist-2 part of the Bjorken sum rule. The derived results were applied for processing of experimental data. We observed a good agreement between the experimental data and the predictions from analytic QCD. In contrast, there is a significant discrepancy between these data and the fitting curves within the standard perturbative approach.

Keywords:

1. Introduction

According to the general principles of (local) quantum field theory (QFT) [1], observables in a spacelike region (i.e. in Euclidean space) can have singularities only for negative values of their argument Q^2. However, for large Q^2 values, these observables are usually represented as power expansions in the running coupling constant (couplant) $\alpha_s(Q^2)$, which has a ghostly singularity, the so-called Landau pole, at $Q^2 = \Lambda^2$. Therefore, to restore the analyticity of the considered expansions, this pole in the strong couplant should be removed.

The strong couplant $\alpha_s(Q^2)$ obeys the renormalization group equation

$$L \equiv \ln \frac{Q^2}{\Lambda^2} = \int^{\overline{a}_s(Q^2)} \frac{da}{\beta(a)}, \quad \overline{a}_s(Q^2) = \frac{\alpha_s(Q^2)}{4\pi} \tag{1}$$

with some boundary condition and the QCD β-function:

$$\beta(a_s) \; = \; -\sum_{i=0} \beta_i \overline{a}_s^{i+2} = -\beta_0 \overline{a}_s^2 \left(1 + \sum_{i=1} b_i a_s^i\right), \quad b_i = \frac{\beta_i}{\beta_0^{i+1}}, \quad a_s(Q^2) = \beta_0 \, \overline{a}_s(Q^2), \tag{2}$$

where

$$\beta_0 = 11 - \frac{2f}{3}, \quad \beta_1 = 102 - \frac{38f}{3}, \quad \beta_2 = \frac{2857}{2} - \frac{5033f}{18} + \frac{325f^2}{54}, \tag{3}$$

 doi:10.20944/preprints202412.1263.v1

for f active quark flavors. Really now the first fifth coefficients, i.e. β_i with $i \leq 4$, are exactly known [2–4]. In our present consideration we will need only $0 \leq i \leq 2$.

Note that in Eq. (2) we have added the first coefficient of the QCD β-function to the a_s definition, as is usually done in the case of analytic couplants (see, e.g., Refs. [5–9]).

So, at the leading order (LO), at the next-to-leading order (NLO) and the next-to-next-to-leading order (NNLO), where $a_s(Q^2) \equiv a_s^{(1)}(Q^2)$, $a_s(Q^2) \equiv a_s^{(2)}(Q^2) = a_s^{(1)}(Q^2) + \delta_s^{(2)}(Q^2)$ and $a_s(Q^2) \equiv a_s^{(3)}(Q^2) = a_s^{(1)}(Q^2) + \delta_s^{(2)}(Q^2) + \delta_s^{(3)}(Q^2)$, respectively, we have from Eq. (1)

$$a_s^{(1)}(Q^2) = \frac{1}{L}, \delta_s^{(2)}(Q^2) = -\frac{b_1 \ln L}{L^2}, \;\; \delta_s^{(3)}(Q^2) = \frac{1}{L^3}\left[b_1^2(\ln^2 L - \ln L - 1) + b_2\right], \tag{4}$$

i.e. $a_s^{(i)}(Q^2)$ $(i = 1, 2, 3)$ contain poles and other singularities at $Q^2 = \Lambda^2$.

In a timelike region ($q^2 > 0$) (i.e., in Minkowski space), the definition of a running couplant turns out to be quite difficult. The reason for the problem is that, strictly speaking, the expansion of perturbation theory (PT) in QCD cannot be defined directly in this region. Since the early days of QCD, much effort has been made to determine the appropriate Minkowski coupling parameter needed to describe important timelike processes such as, e^+e^--annihilation into hadrons, quarkonia and τ-lepton decays into hadrons. Most of the attempts (see, for example, [10]) have been based on the analytical continuation of strong couplant from the deep Euclidean region, where perturbative QCD calculations can be performed, to the Minkowski space, where physical measurements are made. In other developments, analytical expressions for a LO couplant were obtained [11] directly in Minkowski space, using an integral transformation from the spacelike to the timelike mode from the Adler D-function.

In Refs. [5,6] an efficient approach was developed to eliminate the Landau singularity without introducing extraneous infrared controllers, such as the gluon effective mass (see, e.g., [12]). [1] This method is based on a dispersion relation that relates the new analytic couplant $A_{\rm MA}(Q^2)$ to the spectral function $r_{\rm pt}(s)$ obtained in the PT framework. In LO this gives

$$A_{\rm MA}^{(1)}(Q^2) = \frac{1}{\pi}\int_0^{+\infty} \frac{ds}{(s+t)} r_{\rm pt}^{(1)}(s), \;\; r_{\rm pt}^{(1)}(s) = {\rm Im}\, a_s^{(1)}(-s - i\epsilon)\,. \tag{5}$$

The [5,6] approach follows the corresponding results [14] obtained in the framework of Quantum Electrodynamics. Similarly, the analytical images of a running coupling in the Minkowski space are defined using another linear operation

$$\mathcal{U}_{\rm MA}^{(1)}(s) = \frac{1}{\pi}\int_s^{+\infty} \frac{d\sigma}{\sigma} r_{\rm pt}^{(1)}(\sigma)\,, \tag{6}$$

So, we repeat once again: the spectral function in the dispersion relations (5) and (6) is taken directly from PT, and the analytical couplants $A_{\rm MA}(Q^2)$ and $\mathcal{U}_{\rm MA}(Q^2)$ are restored using the corresponding dispersion relations. This approach is usually called the *Minimal Approach* (MA) (see, e.g., [15]) or the *Analytical Perturbation Theory* (APT) [5,6]. [2]

Thus, MA QCD is a very convenient approach that combines the analytical properties of QFT quantities and the results obtained in the framework of perturbative QCD, leading to the appearance of the MA couplants $A_{\rm MA}(Q^2)$ and $\mathcal{U}_{\rm MA}(s)$, which are close to the usual strong couplant $a_s(Q^2)$ in the limit of large Q^2 values and completely different from $a_s(Q^2)$ for small Q^2 values, i.e. for $Q^2 \sim \Lambda^2$.

A further APT development is the so-called fractional APT (FAPT) [7–9], which extends the construction principles described above to PT series, starting from non-integer powers of the couplant.

---

1 Numerically, couplands with effective mass are very close to the analytic one (see [13]).
2 An overview of other similar approaches can be found in [16], including approaches [17] that are close to APT.

 doi:10.20944/preprints202412.1263.v1

In the framework of QFT, such series arise for quantities that have non-zero anomalous dimensions. Compact expressions for quantities within the FAPT framework were obtained mainly in LO, but this approach was also used in higher orders, mainly by re-expanding the corresponding couplants in powers of the LO couplant, as well as using some approximations.

In this review, we show the main properties of MA couplants in the FAPT framework, obtained in Refs. [18,19] using the so-called $1/L$-expansion. Note that for an ordinary couplant, this expansion is applicable only for large Q^2 values, i.e. for $Q^2 >> \Lambda^2$. However, as shown in [18,19], the situation is quite different in the case of analytic couplants, and this $1/L$-expansion is applicable for all values of the argument. This is due to the fact that the non-leading expansion corrections vanish not only at $Q^2 \to \infty$, but also at $Q^2 \to 0$, [3] which leads only to nonzero (small) corrections in the region $Q^2 \sim \Lambda^2$.

Below we consider the representations for the MA couplants and their (fractional) derivatives obtained in [18,19] (see also [20]) and valid in principle in any PT order. However, in order to avoid cumbersome formulas, but at the same time to show the main features of the approach obtained in [18,19], we confine ourselves to considering only the first three PT orders.

Moreover, in this review, we show FAPT applications for the Higgs-boson decay into a bottom-antibottom pair and the description of the polarized Bjorken sum rule (BSR). The results shown here have been recently obtained in Refs. [19] and Refs. [21,22], respetively. In contrast to the formulas, the results for the Higgs boson decay and the polarized Bjorken sum rule will be shown in the first five PT orders, as was obtained in [19,21,22].

The paper is organized as follows. In Section 2 we firstly review the basic properties of the usual strong couplant and its $1/L$-expansion. Section 3 contains fractional derivatives (i.e. ν-derivatives) of the usual strong couplant, which $1/L$-expansions can be represented as some operators acting on the ν-derivatives of the LO strong couplant. In Sections 4 and 5 we present the results for the MA couplands. Section 6 contains formulas conveninet for $Q^2 \sim \Lambda^2$. In Sections 7 and 8 we present the integrals repsenentations for the MA couplands. Sections 9 and 10 contain applications of this approach to the Higgs-boson decay into a bottom-antibottom pair and the Bjorken sum rule, respectively. In conclusion, some final discussions are given. In addition, we have several Appendices, which contain most complicated expressions.

2. Strong Couplant

As shown in the Introduction, the strong couplant $a_s(Q^2)$ obeys the renormalized group equation (1). When $Q^2 >> \Lambda^2$, Eq. (1) can be solved by iterations in the form of a $1/L$-expansion [4] (we give the first three terms of the expansion in accordance with the reasoning in the introduction), which can be represented in the following compact form

$$a_{s,0}^{(1)}(Q^2) = \frac{1}{L_0}, \;\; a_{s,i}^{(i+1)}(Q^2) = a_{s,i}^{(1)}(Q^2) + \sum_{m=2}^{i} \delta_{s,i}^{(m)}(Q^2), \;\; (i = 0, 1, 2, ...), \tag{7}$$

where

$$L_k = \ln t_k, \;\; t_k = \frac{1}{z_k} = \frac{Q^2}{\Lambda_k^2}. \tag{8}$$

The corrections $\delta_{s,k}^{(m)}(Q^2)$ are represented as follows

$$\delta_{s,k}^{(2)}(Q^2) = -\frac{b_1 \ln L_k}{L_k^2}, \;\; \delta_{s,k}^{(3)}(Q^2) = \frac{1}{L_k^3}\left[b_1^2(\ln^2 L_k - \ln L_k - 1) + b_2\right]. \tag{9}$$

---

[3] The absence of high-order corrections for $Q^2 \to 0$ was also discussed in Refs. [5,6].

[4] The $1/L$-expansion gives a good approximation for the solution of Eq. (2) at $Q^2 \geq 10$ GeV^2 (see, for example, [23]).

 doi:10.20944/preprints202412.1263.v1

As shown in Eqs. (7) and (9), in any PT order, the couplant $a_s(Q^2)$ contains its dimensional transmutation parameter Λ, which is related to the normalization of $\alpha_s(M_Z^2)$ as

$$\Lambda_i = M_Z \exp\left\{-\frac{1}{2}\left[\frac{1}{a_s(M_Z^2)} + b_1 \ln a_s(M_Z^2) + \int_0^{\bar{a}_s(M_Z^2)} da \left(\frac{1}{\beta(a)} + \frac{1}{a^2(\beta_0+\beta_1 a)}\right)\right]\right\}, \quad (10)$$

where $\alpha_s(M_Z) = 0.1176$ in PDG20 [24].

2.1. f-Dependence of the Couplant $a_s(Q^2)$.

The coefficients β_i (3) depend on the number f of active quarks that change the couplant $a_s(Q^2)$ at thresholds $Q_f^2 \sim m_f^2$, where some the additional quark comes enters the game $Q^2 > Q_f^2$. Here m_f is the $\overline{MS}$ mass of the f quark, e.g., $m_b = 4.18 + 0.003 - 0.002$ GeV and $m_c = 1.27 \pm 0.02$ GeV from PDG20 [24]. [5] Thus, the couplant a_s depends on f, and this f-dependence can be taken into account in Λ, i.e. it is Λ^f that contributes to the above Eqs. (1) and (7).

Relationships between Λ_i^f and Λ_i^{f-1}, i.e. the so-called matching conditions between $a_s(f, Q_f^2)$ and $a_s(f-1, Q_f^2)$ are known up to the four-loop order [25] in the $\overline{MS}$ scheme and usually are used for $Q_f^2 = m_f^2$, where these relations have the simplest form (see e.g. [26] for a recent review).

Here we will not consider the f-dependence of Λ_i^f and $a_s(f, M_Z^2)$, since we mainly consider the range of small Q^2 values and therefore use $\Lambda_i^{f=3} (i = 0, 1, 2, 3)$ taken from the recent Ref. [27]. Further, since we will consider the $H \to b\bar{b}$ decay as an application, we will use also the results for $\Lambda_i^{f=5}$ taken also from [27] [6]:

$$\begin{aligned} &\Lambda_0^{f=3} = 142 \text{ MeV}, \ \Lambda_1^{f=3} = 367 \text{ MeV}, \ \Lambda_2^{f=3} = 324 \text{ MeV}, \ \Lambda_3^{f=3} = 328 \text{ MeV}, \\ &\Lambda_0^{f=5} = 87 \text{ MeV}, \ \Lambda_1^{f=5} = 224 \text{ MeV}, \ \Lambda_2^{f=5} = 207 \text{ MeV}, \ \Lambda_3^{f=5} = 207 \text{ MeV}. \end{aligned} \quad (11)$$

We use also $\Lambda_4 = \Lambda_3$, since in highest orders Λ_i values become very similar.

In Figure 1 one can see that the strong couplants $a_{s,i}^{(i+1)}(Q^2)$ become to be singular at $Q^2 = \Lambda_i^2$. The values of Λ_0 and Λ_j $(j \geq 1)$ are very different (see Eq. (11) below): the values of $(\Lambda_i^{f=3})^2$ $(i = 0, 2, 4)$ are also shown in Figure 1 vertical lines.

---

[5] Strictly speaking, the quark masses in the $\overline{MS}$ scheme depend on Q^2 and $m_f = m_f(Q^2 = m_f^2)$. The Q^2-dependence is rather slow and will not be discussed in this paper.

[6] The [27] authors used the result of PDG20 $\alpha_s(M_Z) = 0.1179(10)$. Now there is also the result PDG21 $\alpha_s(M_Z) = 0.1179(9)$ which contains the same center value. Note that very close numerical relationships between Λ_i were also obtained by [28] for $\alpha_s(M_Z) = 0.1168(19)$ extracted by the ZEUS collaboration (see [29]).

Preprints.org (www.preprints.org) | NOT PEER-REVIEWED | Posted: 16 December 2024 doi:10.20944/preprints202412.1263.v1

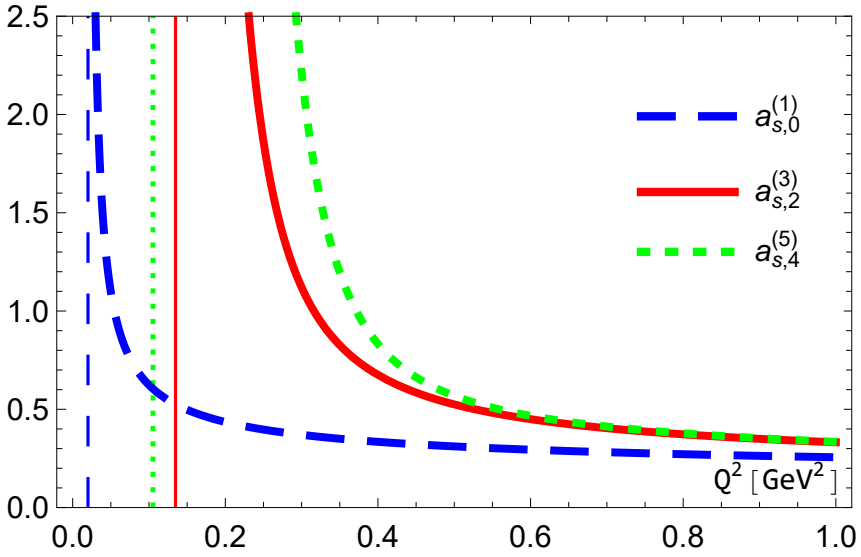

Figure 1. The results for $a_{s,i}^{(i+1)}(Q^2)$ and $(\Lambda_i^{f=3})^2$ (vertical lines) with $i = 0, 2, 4$. Here and in the following figures, the $\Lambda_i^{f=3}$ values shown in (11) are used.

3. Fractional Derivatives

Following [30,31], we introduce the derivatives (in the (i)-order of of PT)

$$\tilde{a}_{n+1}^{(i)}(Q^2) = \frac{(-1)^n}{n!}\,\frac{d^n a_s^{(i)}(Q^2)}{(dL)^n}\,, \tag{12}$$

which are very convenient in the case of the analytical QCD (see, e.g., [32]).

The series of derivatives $\tilde{a}_n(Q^2)$ can successfully replace the corresponding series of a_s-degrees. Indeed, each the derivative reduces the a_s degree, but is accompanied by an additional β-function $\sim a_s^2$. Thus, each application of a derivative yields an additional a_s, and thus indeed possible to use series of derivatives instead of series of a_s-powers.

In LO, the series of derivatives $\tilde{a}_n(Q^2)$ are exactly the same as a_s^n. Beyond LO, the relationship between $\tilde{a}_n(Q^2)$ and a_s^n was established in [31,33] and extended to fractional cases, where $n \to$ is a non-integer ν, in Ref. [34].

Now consider the $1/L$-expansion of $\tilde{a}_\nu^{(k)}(Q^2)$. We can raise the ν-power of the results (7) and (9) and then restore $\tilde{a}_\nu^{(k)}(Q^2)$ using the relations between $\tilde{a}_\nu$ and a_s^ν obtained in [34] (see Appendix A) This operation is carried out in more details in Appendix B to [18] (see also Appendix A to [20]). Here we present only the final results, which have the form [7]:

$$\tilde{a}_{\nu,0}^{(1)}(Q^2) = \left(a_{s,0}^{(1)}(Q^2)\right)^\nu = \frac{1}{L_0^\nu},\ \tilde{a}_{\nu,i}^{(i+1)}(Q^2) = \tilde{a}_{\nu,i}^{(1)}(Q^2) + \sum_{m=1}^{i} C_m^{\nu+m}\,\tilde{\delta}_{\nu,i}^{(m+1)}(Q^2),$$
$$\tilde{\delta}_{\nu,i}^{(m+1)}(Q^2) = \hat{R}_m\,\frac{1}{L_i^{\nu+m}},\ C_m^{\nu+m} = \frac{\Gamma(\nu+m)}{m!\Gamma(\nu)}\,, \tag{13}$$

where

$$\hat{R}_1 = b_1\left[\hat{Z}_1(\nu) + \frac{d}{d\nu}\right],\ \hat{R}_2 = b_2 + b_1^2\left[\frac{d^2}{(d\nu)^2} + 2\hat{Z}_1(\nu+1)\frac{d}{d\nu} + \hat{Z}_2(\nu+1)\right] \tag{14}$$

and $\hat{Z}_j(\nu)$ $(j = 1, 2)$ are combinations of the Euler Ψ-functions and their derivatives.

---

[7] The expansion (13) is similar to those used in Refs. [7,8] for the expansion of $\left(a_{s,i}^{(i+1)}(Q^2)\right)^\nu$ in terms of powers of $a_{s,i}^{(1)}(Q^2)$.

 doi:10.20944/preprints202412.1263.v1

The representation (13) of the $\tilde{\delta}^{(m+1)}_{\nu,i}(Q^2)$ corrections as $\hat{R}_m$-operators is very important[8] and allows us to similarly present high-order results for the ($1/L$-expansion) of analytic couplants.

4. MA Couplings

We first show the LO results, and then go beyond LO following our results (13) for the ordinary strong couplant obtained in the previous section.

4.1. LO

The LO MA couplant $A^{(1)}_{\mathrm{MA},\nu,0}$ has the following form [7]

$$A^{(1)}_{\mathrm{MA},\nu,0}(Q^2) = \left(a^{(1)}_{\nu,0}(Q^2)\right)^{\nu} - \frac{\mathrm{Li}_{1-\nu}(z_0)}{\Gamma(\nu)} = \frac{1}{L_0^{\nu}} - \frac{\mathrm{Li}_{1-\nu}(z_0)}{\Gamma(\nu)} \equiv \frac{1}{L_0^{\nu}} - \Delta^{(1)}_{\nu,0}\,, \tag{15}$$

where

$$\mathrm{Li}_{\nu}(z) = \sum_{m=1}^{\infty} \frac{z^m}{m^{\nu}} = \frac{z}{\Gamma(\nu)} \int_0^{\infty} \frac{dt\; t^{\nu-1}}{(e^t - z)} \tag{16}$$

is the Polylogarithm.

The LO MA couplant $U^{(1)}_{\mathrm{MA},\nu,0}$ in the Minkowski space has the form [8]

$$U^{(1)}_{\mathrm{MA},\nu,0}(\mathrm{s}) = \frac{\sin[(\nu-1)\, g_0(s)]}{\pi(\nu-1)(\pi^2 + L^2_{s,0})^{(\nu-1)/2}}\,, \; (\nu > 0)\,, \tag{17}$$

where

$$L_{s,i} = \ln \frac{s}{\Lambda_i^2}, \;\; g_i(s) = \arccos\left(\frac{L_{s,i}}{\sqrt{\pi^2 + L^2_{s,i}}}\right). \tag{18}$$

For $\nu = 1$ we recover the famous Shirkov-Solovtsov results [5]:

$$A^{(1)}_{\mathrm{MA},0}(Q^2) \equiv A^{(1)}_{\mathrm{MA},^\circ=1,0}(Q^2) = \frac{1}{L_0} - \frac{z_0}{1-z_0}, \; U^{(1)}_{\mathrm{MA},0}(Q^2) \equiv U^{(1)}_{\mathrm{MA},^\circ=1,0}(\mathrm{s}) = \frac{g_0(s)}{\pi}\,. \tag{19}$$

Note that the result (19) can be taken directly for the integral forms (5) and (6), as it was in Ref. [5].

4.2. Beyond LO

Following Eqs. (15) and (17) for the LO analytic couplants, we consider the derivatives of the MA couplants, as

$$\tilde{A}_{\mathrm{MA},n+1}(Q^2) = \frac{(-1)^n}{n!} \frac{d^n A_{\mathrm{MA}}(Q^2)}{(dL)^n}, \;\; \tilde{U}_{\mathrm{MA},n+1}(Q^2) = \frac{(-1)^n}{n!} \frac{d^n U_{\mathrm{MA}}(s)}{(dL_s)^n}\,. \tag{20}$$

By analogy with ordinary couplant, using the results (13) we have for MA analytic couplants $\tilde{A}^{(i+1)}_{\mathrm{MA},\nu,i}$ and $\tilde{U}^{(i+1)}_{\mathrm{MA},\nu,i}$ the following expressions:

$$\begin{aligned} \tilde{A}^{(i+1)}_{\mathrm{MA},\nu,i}(Q^2) &= \tilde{A}^{(1)}_{\mathrm{MA},\nu,i}(Q^2) + \sum_{m=1}^{i} C^{\nu+m}_m \tilde{\delta}^{(m+1)}_{\mathrm{A},\nu,i}(Q^2), \\ \tilde{U}^{(i+1)}_{\mathrm{MA},\nu,i}(s) &= \tilde{U}^{(1)}_{\mathrm{MA},\nu,i}(s) + \sum_{m=1}^{i} C^{\nu+m}_m \tilde{\delta}^{(m+1)}_{\mathrm{U},\nu,i}(s), \end{aligned} \tag{21}$$

---

[8] The results for $\hat{R}_m$-operators contain the transcendental principle [35]: the corresponding functions $\hat{Z}_k(\nu)$ ($k \le m$) contain the Polygamma-functions $\Psi_k(\nu)$ and their products, such as $\Psi_{k-l}(\nu)\Psi_l(\nu)$, and also with a larger number of factors) with the same total index k. However, the importance of this property is not clear yet.

 doi:10.20944/preprints202412.1263.v1

where $\tilde{A}^{(1)}_{\mathrm{MA},\nu,i}$ and $\tilde{U}^{(1)}_{\mathrm{MA},\nu,i}$ are given in Eqs. (15) and (17), respectively, and

$$\tilde{\delta}^{(m+1)}_{\mathrm{A},\nu,i}(Q^2) = \tilde{\delta}^{(m+1)}_{\nu,i}(Q^2) - \hat{R}_m\left(\frac{\mathrm{Li}_{-\nu-m+1}(z_i)}{\Gamma(\nu+m)}\right),\ \tilde{\delta}^{(m+1)}_{\mathrm{U},\nu,i}(s) = \hat{R}_m\left(\tilde{U}^{(1)}_{\mathrm{MA},\nu+m,i}(s)\right). \tag{22}$$

and $\tilde{\delta}^{(m+1)}_{\nu,i}(Q^2)$ and $\hat{R}_m$ are given in Eqs. (13) and (14), respectively.

The relations (15) reflect the fact that the MA procedure (15) and the operation $d/(d\nu)$ commute. Thus, to obtain (15) we propose that the form (13) for the usual couplant a_s at high orders is exactly applicable (exactly in the same way) also to the case of the (MA) couplant.

Spacelike case. After some evaluations, we obtain the following expressions without operators

$$\tilde{\Delta}^{(i+1)}_{\nu,i} = \tilde{\Delta}^{(1)}_{\nu,i} + \sum_{m=1}^{i} C^{\nu+m}_{m}\,\overline{R}_m(z_i)\left(\frac{\mathrm{Li}_{-\nu-m+1}(z_i)}{\Gamma(\nu+m)}\right), \tag{23}$$

where

$$\begin{aligned}
&\overline{R}_1(z) = b_1\Big[\gamma_{\mathrm{E}} - 1 + \mathrm{M}_{-\nu,1}(z)\Big],\\
&\overline{R}_2(z) = b_2 + b_1^2\Big[\mathrm{M}_{-\nu-1,2}(z) + 2(\gamma_{\mathrm{E}}-1)\mathrm{M}_{-\nu-1,1}(z) + (\gamma_{\mathrm{E}}-1)^2 - \zeta_2\Big]
\end{aligned} \tag{24}$$

and

$$\mathrm{Li}_{\nu,k}(z) = (-1)^k\frac{d^k}{(d\nu)^k}\mathrm{Li}_{\nu}(z) = \sum_{m=1}^{\infty}\frac{z^m\ln^k m}{m^{\nu}},\ \ \mathrm{M}_{\nu,k}(z) = \frac{\mathrm{Li}_{\nu,k}(z)}{\mathrm{Li}_{\nu}(z)}. \tag{25}$$

We see that the $\Psi(\nu)$-function and its derivatives have completely canceled out. Note that another form for $\tilde{\Delta}^{(m+1)}_{\nu,i}(Q^2)$ is given in Appendix C.

So, we have for MA analytic couplants $\tilde{A}^{(i+1)}_{\mathrm{MA},\nu}$ the following expressions:

$$\tilde{A}^{(i+1)}_{\mathrm{MA},\nu,i}(Q^2) = \tilde{A}^{(1)}_{\mathrm{MA},\nu,i}(Q^2) + \sum_{m=1}^{i} C^{\nu+m}_{m}\,\tilde{\delta}^{(m+1)}_{\mathrm{A},\nu,i}(Q^2) \tag{26}$$

where

$$\begin{aligned}
&\tilde{A}^{(1)}_{\mathrm{A},\nu,i}(Q^2) = \tilde{a}^{(1)}_{\nu,i}(Q^2) - \frac{\mathrm{Li}_{1-\nu}(z_i)}{\Gamma(\nu)},\\
&\tilde{\delta}^{(m+1)}_{\mathrm{A},\nu,i}(Q^2) = \tilde{\delta}^{(m+1)}_{\nu,i}(Q^2) - \overline{R}_m(z_i)\,\frac{\mathrm{Li}_{-\nu+1-m}(z_i)}{\Gamma(\nu+m)}
\end{aligned} \tag{27}$$

and $\tilde{\delta}^{(k+1)}_{\nu,m}(Q^2)$ are given in Eq. (13).

Timelike case. Using the results (13) for the usual couplant we have

$$\begin{aligned}
&\tilde{U}^{\mathrm{MA},(i+1)}_{\nu}(\mathrm{s}) = \tilde{U}^{(1)}_{\mathrm{MA},\nu}(\mathrm{s}) + \sum_{m=1}^{i} C^{\nu+m}_{m}\,\tilde{\delta}^{(m+1)}_{\mathrm{U},\nu}(\mathrm{s}),\\
&\tilde{\delta}^{(m+1)}_{\mathrm{U},\nu}(\mathrm{s}) = \hat{R}_m\,\tilde{U}^{(1)}_{\mathrm{MA},\nu+m}(\mathrm{s}),
\end{aligned} \tag{28}$$

where $\tilde{U}^{(1)}_{\mathrm{MA},\nu}(\mathrm{s})$ is given in Eq. (17).

This approach allows to express the high order corrections in explicit form

$$\tilde{\delta}^{(m+2)}_{\mathrm{U},\nu}(\mathrm{s}) = \frac{1}{(\nu+m)\pi(\pi^2+L_s^2)^{(\nu+m)/2}}\Big\{\bar{\delta}^{(m+2)}_{\nu+m-1}(\mathrm{s})\sin\big((\nu+m)g\big) + \hat{\delta}^{(m+2)}_{\nu+m-1}(\mathrm{s})g\cos\big((\nu+m)g\big)\Big\}, \tag{29}$$

 doi:10.20944/preprints202412.1263.v1

where $\overline{\delta}_\nu^{(m+2)}(\mathrm{s})$ and $\hat{\delta}_\nu^{(m+2)}(\mathrm{s})$ are

$$\begin{aligned}
&\overline{\delta}_\nu^{(2)}(\mathrm{s}) = b_1\left[\hat{Z}_1(\nu) - G\right],\ \hat{\delta}_\nu^{(2)}(\mathrm{s}) = b_1\,,\\
&\overline{\delta}_\nu^{(3)}(\mathrm{s}) = b_2 + b_1^2\left[\hat{Z}_2(\nu) - 2G\hat{Z}_1(\nu) + G^2 - g^2\right],\ \hat{\delta}_\nu^{(3)}(\mathrm{s}) = 2b_1^2\left[\hat{Z}_1(\nu) - G\right]
\end{aligned} \tag{30}$$

and

$$G(\mathrm{s}) = \frac{1}{2}\,\ln\!\left(\pi^2 + L_s^2\right). \tag{31}$$

4.3. The Case $\nu = 1$

Here we present only the results for the case $\nu = 1$:

$$\begin{aligned}
&A_{\mathrm{MA},i}^{(i+1)}(Q^2) \equiv \tilde{A}_{\mathrm{MA},\nu=1,i}^{(i+1)}(Q^2) = A_{\mathrm{MA},i}^{(1)}(Q^2) + \sum_{m=1}^{i}\tilde{\delta}_{\mathrm{A},\nu=1,i}^{(m+1)}(Q^2),\\
&U_{\mathrm{MA},i}^{(i+1)}(s) \equiv \tilde{U}_{\mathrm{MA},\nu=1,i}^{(i+1)}(s) = U_{\mathrm{MA},i}^{(1)}(s) + \sum_{m=1}^{i}\tilde{\delta}_{\mathrm{U},\nu=1,i}^{(m+1)}(s)
\end{aligned} \tag{32}$$

where $A_{\mathrm{MA},i}^{(1)}(Q^2)$ and $U_{\mathrm{MA},i}^{(1)}(s)$ are shown in Eq. (19) and

$$\begin{aligned}
&\tilde{\delta}_{\mathrm{A},\nu=1,i}^{(m+1)}(Q^2) = \tilde{\delta}_{\nu=1,i}^{(m+1)}(Q^2) - \frac{P_{m,1}(z_i)}{m!}\,,\\
&\tilde{\delta}_{\mathrm{A},\nu=1,i}^{(2)}(\mathrm{s}) = \frac{b_1}{\pi(\pi^2 + L_{s,i}^2)^{1/2}}\Big\{g_i\cos(g_i) - \left[1 + G_i\right]\sin(g_i)\Big\},\\
&\tilde{\delta}_{\mathrm{U},\nu=1,i}^{(3)}(\mathrm{s}) = \frac{1}{2\pi(\pi^2 + L_s^2)}\left(b_2\sin(2g_i) + b_1^2\Big[G_i^2 - g_i^2 - 1\Big]\sin(2g_i)\right)
\end{aligned} \tag{33}$$

with

$$\begin{aligned}
&G_i(\mathrm{s}) = \frac{1}{2}\,\ln\!\left(\pi^2 + L_{s,i}^2\right),\ P_{1,\nu}(z) = b_1\left[\overline{\gamma}_{\mathrm{E}}\mathrm{Li}_{-\nu}(z) + \mathrm{Li}_{-\nu,1}(z)\right],\ \overline{\gamma}_{\mathrm{E}} = \gamma_{\mathrm{E}} - 1,\\
&P_{2,\nu}(z) = b_2\,\mathrm{Li}_{-\nu-1}(z) + b_1^2\Big[\mathrm{Li}_{-\nu-1,2}(z) + 2\overline{\gamma}_{\mathrm{E}}\mathrm{Li}_{-\nu-1,1}(z) + \left(\overline{\gamma}_{\mathrm{E}}^2 - \zeta_2\right)\mathrm{Li}_{-\nu-1}(z)\Big]\,,
\end{aligned} \tag{34}$$

Euler constant γ_{E} and

$$\mathrm{Li}_{n,m}(z) = \sum_{m=1}\frac{\ln^k m}{m^n},\ \mathrm{Li}_{-1}(z) = \frac{z}{(1-z)^2},\ \mathrm{Li}_{-2}(z) = \frac{z(1+z)}{(1-z)^3}\,. \tag{35}$$

Using the results in Eq. (18) and transformation rules for $\sin(ng)$ and $\cos(ng)$, we have

$$\sin(ng) = \frac{S(ng)}{(\pi^2 + L_s^2)^{n/2}},\ \ \cos(ng) = \frac{C(ng)}{(\pi^2 + L_s^2)^{n/2}}, \tag{36}$$

where

$$\begin{aligned}
&S(g) = \pi,\ C(g) = L_s,\ S(2g) = 2\pi L_s,\ C(2g) = L_s^2 - \pi^2,\ S(3g) = \pi(3L_s^2 - \pi^2),\\
&C(3g) = L_s(L_s^2 - 3\pi^2)\,.
\end{aligned} \tag{37}$$

 doi:10.20944/preprints202412.1263.v1

Using Eqs. (36) and (37), the results for $\tilde{\delta}^{(m+1)}_{\mathrm{U},\nu=1}(\mathrm{s})$ in (29) can be rewritten in the following form

$$\tilde{\delta}^{(2)}_{\mathrm{U},\nu=1}(\mathrm{s}) = \frac{b_1}{(\pi^2+L_s^2)}\Big(\frac{g}{\pi}L_s - (1+G)\Big),$$
$$\tilde{\delta}^{(3)}_{\mathrm{U},\nu=1}(\mathrm{s}) = \frac{1}{(\pi^2+L_s^2)^2}\Big[b_2 L_s - b_1^2\Big(\frac{gG}{\pi}(L_s^2-\pi^2) + L_s\big(1+g^2-G^2\big)\Big)\Big], \tag{38}$$

which is similar to the results for the spectral function $r_1^{(i)}(\mathrm{s})$ done in ref.[36,37] (see also Section 6 in [18]).

5. The Behaviour of MA Couplings

Here we show the behavious of the MA couplands $A^{(k+1)}_{\mathrm{MA},k}(Q^2) = \tilde{A}^{(k+1)}_{\mathrm{MA},\nu=1,k}(Q^2)$ and $U^{(k+1)}_{\mathrm{MA},k}(s) = \tilde{U}^{(k+1)}_{\mathrm{MA},\nu=1,k}(s)$ and compare them.

5.1. Coupland $\tilde{A}^{(k+1)}_{\mathrm{MA},\nu,k}(Q^2)$

From Figures 2 and 3 we can see differences between $A^{(i+1)}_{\mathrm{MA},^\circ=1,\mathrm{i}}(Q^2)$ with $i = 0,2,4$, which are rather small and have nonzero values around the position $Q^2 = \Lambda_i^2$. In Figure 2 the values of $(\Lambda_i^{f=3})^2$ $(i = 0,2,4)$ are shown by vertical lines (as in Figure 1).

Figure 4 show the results for $A^{(1)}_{\mathrm{MA},^\circ,0}(Q^2)$ and $A^{(2)}_{\mathrm{MA},^\circ,1}(Q^2)$ and their difference $\delta^{(2)}_{\mathrm{A},^\circ,1}(Q^2)$, which is essentially less then the couplants theirselves. From Figure 4 it is clear that for $Q^2 \to 0$ the asymptotic behaviors of $A^{(1)}_{\mathrm{MA},^\circ,0}(Q^2)$, $A^{(2)}_{\mathrm{MA},^\circ,1}(Q^2)$ and $A^{(3)}_{\mathrm{MA},^\circ,2}(Q^2)$ coincide, i.e. the differences $\delta^{(2)}_{\mathrm{A},^\circ=1,1}(Q^2 \to 0)$ and $\delta^{(3)}_{\mathrm{A},^\circ=1,2}(Q^2 \to 0)$ are negligible. Also Figure 5 shows the differences $\delta^{(i+1)}_{\mathrm{A},^\circ=1,\mathrm{i}}(Q^2)$ $(i \geq 2)$ essentially less then $\delta^{(2)}_{\mathrm{A},^\circ=1,1}(Q^2)$.

Thus, we can conclude that contrary to the case of the usual couplant, considered in Figure 1, the $1/L$-expansion of the MA couplant is very good approximation at any Q^2 values. Moreover, the differences between $A^{(i+1)}_{\mathrm{MA},^\circ=1,\mathrm{i}}(Q^2)$ and $A^{(1)}_{\mathrm{MA},^\circ=1,0}(Q^2)$ are small. So, the expansions of $A^{(i+1)}_{\mathrm{MA},^\circ=1,\mathrm{i}}(Q^2)$ $i \geq 1$ through the one $A^{(1)}_{\mathrm{MA},^\circ=1,0}(Q^2)$ done in Refs. [7–9] are very good approximations. Also the approximation

$$A^{(i+1)}_{\mathrm{MA},^\circ=1,\mathrm{i}}(Q^2) = A^{(1)}_{\mathrm{MA},^\circ=1,0}(k_i Q^2), \quad (i = 1,2)\,, \tag{39}$$

introduced in [38,39] and used in [40] is very convenient, too. Indeed, since the corrections $\delta^{(i+1)}_{\mathrm{MA},^\circ=1,\mathrm{i}}(Q^2)$ are very small, then for example from Eq. (33) one can see that the MA couplants $A^{(i+1)}_{\mathrm{MA},^\circ=1,\mathrm{i}}(Q^2)$ are very similar to the LO ones taken with the corresponding Λ_i.

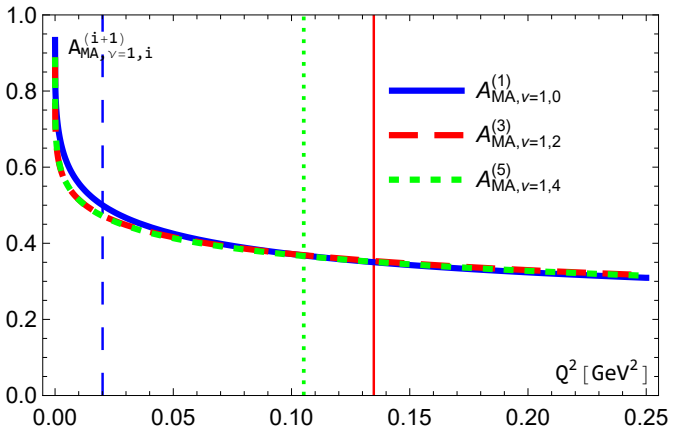

Figure 2. The results for $A^{(i+1)}_{\mathrm{MA},^\circ=1,\mathrm{i}}(Q^2)$ and $(\Lambda_i^{f=3})^2$ (vertical lines) with $i = 0,2,4$.

Preprints.org (www.preprints.org) | NOT PEER-REVIEWED | Posted: 16 December 2024 doi:10.20944/preprints202412.1263.v1

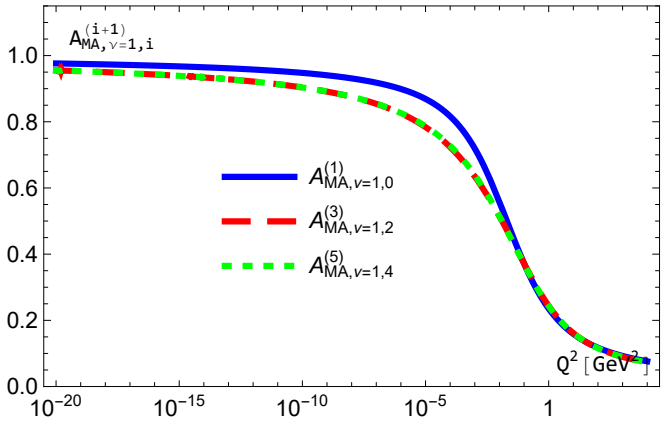

Figure 3. The results for $A^{(i+1)}_{\mathrm{MA},^\circ=1,\mathrm{i}}(Q^2)$ $(i = 0, 1, 2)$ but with the logarithmic scale.

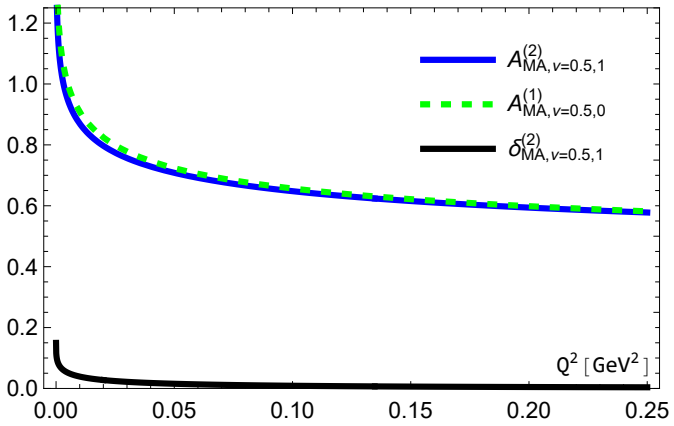

Figure 4. The results for $A^{(1)}_{\mathrm{MA},^\circ=0.5,0}(Q^2)$, $A^{(2)}_{\mathrm{MA},^\circ=0.5,1}(Q^2)$ and $\delta^{(2)}_{\mathrm{A},^\circ=0.5,1}(Q^2)$.

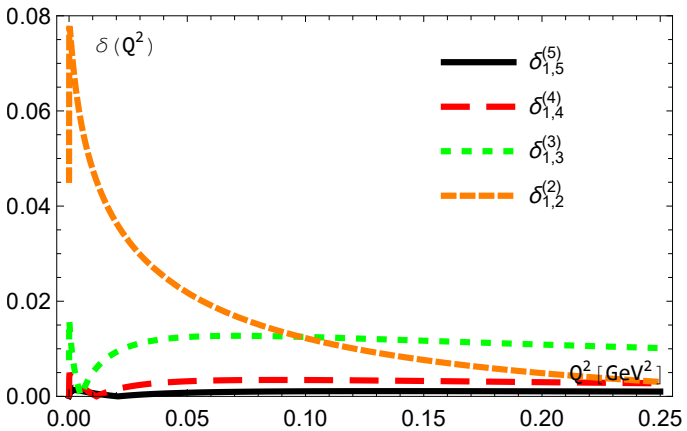

Figure 5. The results for $\delta^{(i+1)}_{\mathrm{A},^\circ=1,\mathrm{i}}(Q^2)$ with $i = 1, 2, 3, 4$.

5.2. Coupland $\tilde{U}^{(k+1)}_{\mathrm{MA},\nu,k}(Q^2)$

This subsection provides graphical results of couplant construction. Figures 6 and 7 show the results for $U^{(i)}_{\mathrm{MA},^\circ=1}(s)$ with $i = 1, 3, 5$ in usual and logarithmic scales (the last one was chosen to stress the limit $U^{(i)}_{\mathrm{MA},^\circ=1}(s \to 0) \to 1$). From Figures 8 and 9 we can see the differences between

Preprints.org (www.preprints.org) | NOT PEER-REVIEWED | Posted: 16 December 2024 doi:10.20944/preprints202412.1263.v1

$U^{(i)}_{\mathrm{MA},^\circ=1}(Q^2)$ with $i = 1,..,5$, which are rather small and have nonzero values around the position $Q^2 = \Lambda_i^2$.

So, Figures 6–9 point out that the difference between $U^{(i+1)}_{\mathrm{MA},^\circ=1}(s)$ and $U^{(i)}_{\mathrm{MA},^\circ=1}(s)$ is essentially less then the couplants themselves. From Figures 7–9 it is clear that for $s \to 0$ the asymptotic behavior of $U^{(1)}_{\mathrm{MA},^\circ=1}(s)$, $U^{(3)}_{\mathrm{MA},^\circ=1}(s)$ and $U^{(5)}_{\mathrm{MA},^\circ=1}(s)$ coincides, i.e. the differences $\delta^{(i)}_{\mathrm{U},^\circ=1}(s \to 0)$ are negligible. Also Figures 8 and 9 show the differences $\delta^{(i+1)}_{\mathrm{U},^\circ=1}(s)$ $(i \geq 2)$ essentially less then $\delta^{(2)}_{\mathrm{U},^\circ=1}(s)$. We note that general form of the results is exactly the same as in the case of the MA couplants $A^{(i+1)}_{\mathrm{MA},^\circ,\mathrm{i}}(Q^2)$, which have been studied in the previous subsection.

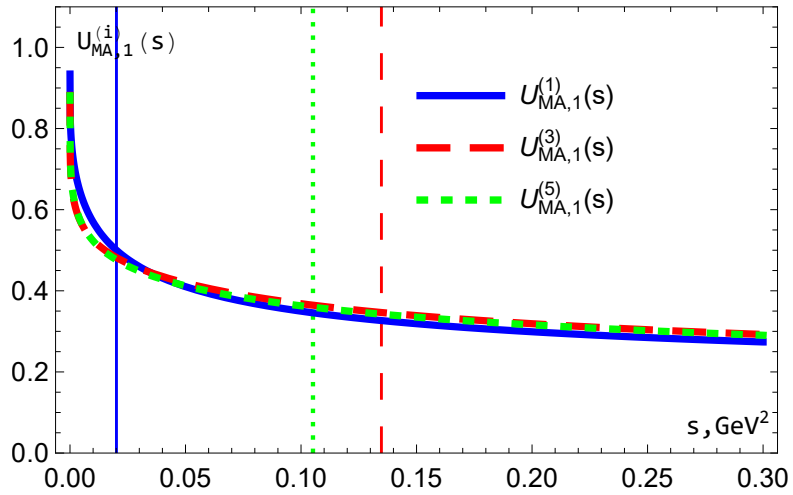

Figure 6. 1,3 and 5 orders of $U^{(i)}_{\mathrm{MA},\nu=1}$ .The vertical lines indicate $(\Lambda^{f=3}_{i-1})^2$

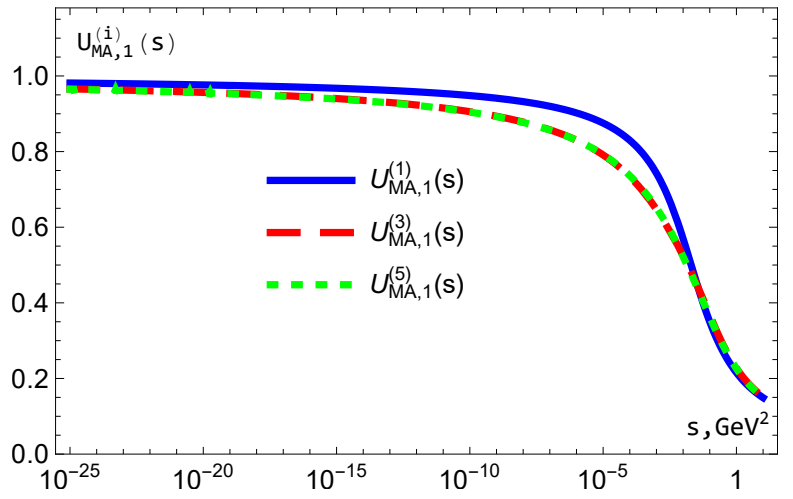

Figure 7. 1,3 and 5 orders of $U^{(i)}_{\mathrm{MA},\nu=1}$ with logarithmic scale of s

Preprints.org (www.preprints.org) | NOT PEER-REVIEWED | Posted: 16 December 2024 doi:10.20944/preprints202412.1263.v1

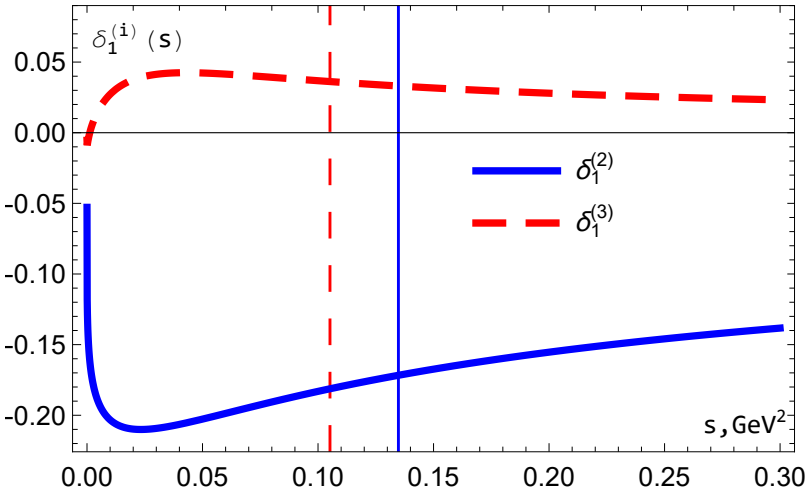

Figure 8. $\delta^{(i)}_{\mathrm{MA},\nu=1}$ with $i = 2, 3$.The vertical lines indicate $(\Lambda^{f=3}_{i-1})^2$

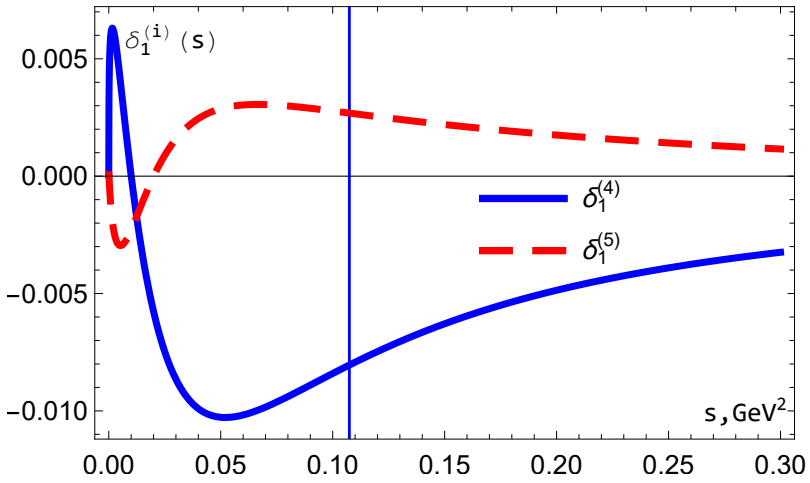

Figure 9. $\delta^{(i)}_{\mathrm{U},\nu=1}$ with $i = 4, 5$. The vertical line indicates $(\Lambda^{f=3}_3)^2 = \Lambda^{f=3}_4)^2$

5.3. Couplands $\tilde{A}^{(k+1)}_{\mathrm{MA},\nu,k}(Q^2)$ *and* $\tilde{U}^{(k+1)}_{\mathrm{MA},\nu,k}(Q^2)$

On Figure 10 we see that $A^{(i+1)}_{\mathrm{MA,i}}(Q^2)$ and $U^{(i+1)}_{\mathrm{MA,i}}(Q^2)$ are very close to each other for $i = 0$ and $i = 2$. The differences between the L0 and NNLO results are nonzero only for $Q^2 \sim \Lambda^2$.

Preprints.org (www.preprints.org) | NOT PEER-REVIEWED | Posted: 16 December 2024 doi:10.20944/preprints202412.1263.v1

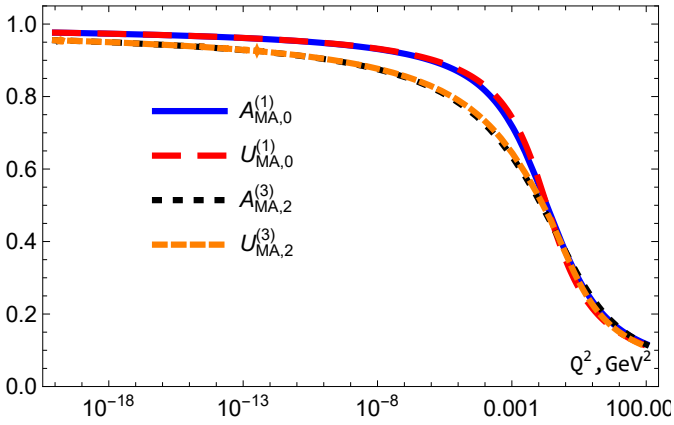

Figure 10. The results for $A^{(i+1)}_{\mathrm{MA,i}}(Q^2)$ and $U^{(i+1)}_{\mathrm{MA,i}}(Q^2)$ with $i = 0, 2$.

Indeed, the similarity is shown in Figures 11 and 12. In Figure 11 the results for $U^{(i)}_{\mathrm{MA},^\circ=1}(s)$ and $A^{(i)}_{\mathrm{MA},^\circ=1}(Q^2)$ ($i = 1, 3, 5$) are shown in the so-called mirror form, which is in accordance with the similar one presented earlier in [8]. Figure 12 contains $U^{(1)}_{\mathrm{MA},^\circ=1}(s)$, $A^{(1)}_{\mathrm{MA},^\circ=1}(Q^2)$, $U^{(2)}_{\mathrm{MA},^\circ=1}(s)$ and $A^{(2)}_{\mathrm{MA},^\circ=1}(Q^2)$ which are very close to each others but have different limit values when $Q^2 \to 0$. Moreover, the differences $\delta^{(2)}_{\mathrm{A},^\circ=1}(Q^2)$ and $\delta^{(2)}_{\mathrm{U},^\circ=1}(Q^2)$ are almost the same although correction of the spacelike couplant decreases more rapidly. The direct relation between $A^{(i)}_{\mathrm{MA},^\circ=1}(Q^2)$ and $U^{(i)}_{\mathrm{MA},^\circ=1}(Q^2)$ gives an interesting picture (see Figure 13). Obviously we have $\frac{A^{(i)}_{\mathrm{MA},^\circ=1}(Q^2=0)}{U^{(i)}_{\mathrm{MA},^\circ=1}(Q^2=0)} = 1$ for any order and the second similar point

$$\frac{A^{(i)}_{\mathrm{MA},^\circ=1}(Q^2 = (\Lambda^{f=3}_{i-1})^2)}{U^{(i)}_{\mathrm{MA},^\circ=1}(Q^2 = (\Lambda^{f=3}_{i-1})^2)} = 1 \tag{40}$$

for $i = 1$. Higher order corrections break the identity (40), shifting the second point from $(\Lambda^{f=3}_i)^2$. As we can see in Figure 13, the shift is quite small. As can be seen from Figure 13, the ratio (40) asymptotically approaches 1 when $Q^2 \to \infty$.

In Figures 6, 8, 9 and 13 the values of $(\Lambda^{f=3}_i)^2$ ($i = 0, 2, 4$) are shown by vertical lines with color matching in each order. Note that Figure 9 contains only one vertical line since $(\Lambda^{f=3}_4)^2 = (\Lambda^{f=3}_5)^2$.

Thus, we can conclude that contrary to the case of the usual couplant, the $1/L$-expansion of the MA couplant is very good approximation at any $Q^2(s)$ values. Moreover, the differences between $U^{(i+1)}_{\mathrm{MA},^\circ=1}(s)$ and $U^{(i)}_{\mathrm{MA},^\circ=1}(s)$ become smaller with the increase of order. So, the expansions of $U^{(i+1)}_{\mathrm{MA},^\circ=1}(s)$ $i \geq 1$ through the $U^{(1)}_{\mathrm{MA},^\circ=1}(s)$ done in Refs. [7–9] are very good approximations.

Preprints.org (www.preprints.org) | NOT PEER-REVIEWED | Posted: 16 December 2024 doi:10.20944/preprints202412.1263.v1

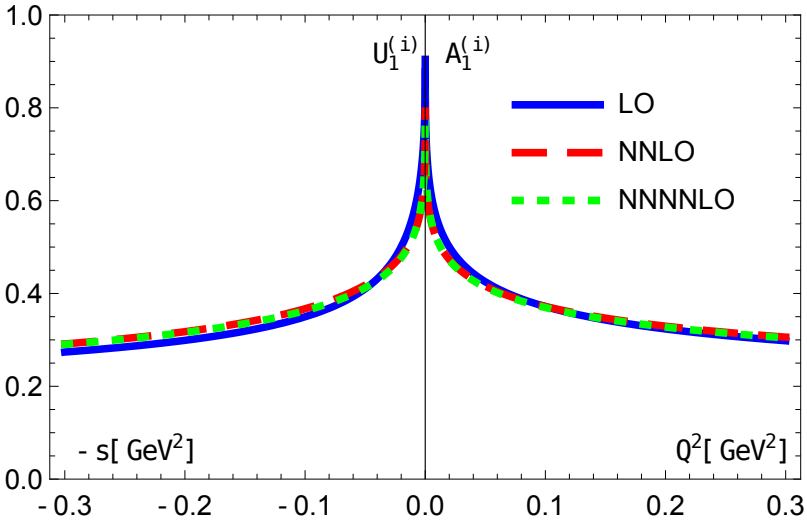

Figure 11. 1,3 and 5 orders of $U^{(i)}_{\mathrm{MA},\nu=1}$ and $A^{(i)}_{\mathrm{MA},\nu=1}$

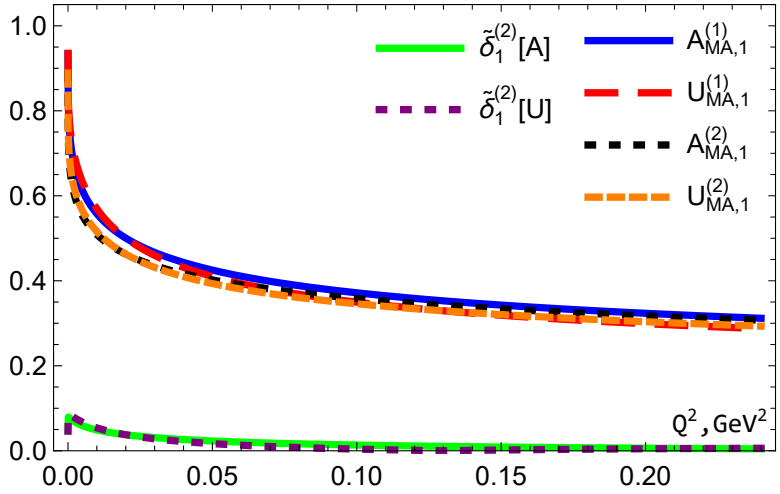

Figure 12. 1 and 2 orders of $U^{(i)}_{\mathrm{MA},\nu=1}$, $A^{(i)}_{\mathrm{MA},\nu=1}$ and $\delta^{(2)}_{\mathrm{MA},\nu=1}$ in Euclidean and Minkowki spaces.

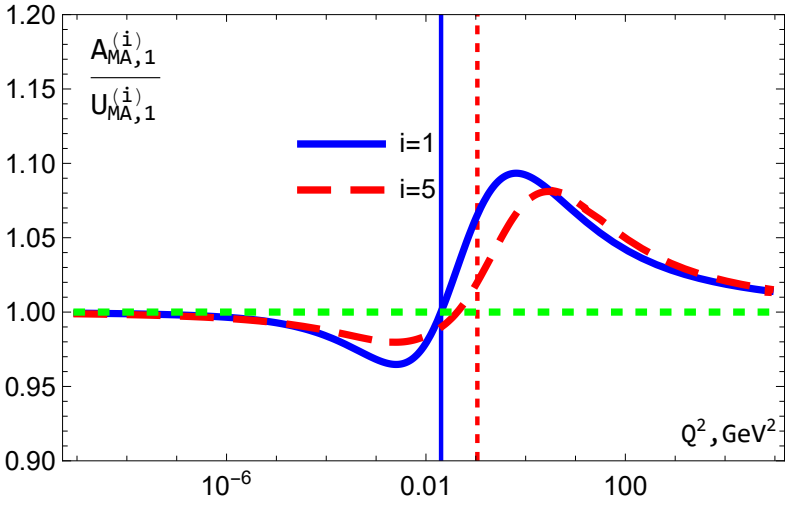

Figure 13. The relation $A^{(i)}_{\mathrm{MA},^\circ=1}/U^{(i)}_{\mathrm{MA},^\circ=1}$ for $i=1,5$. The vertical lines indicate $(\Lambda^{f=3}_{i-1})^2$.

 doi:10.20944/preprints202412.1263.v1

6. MA Coupling $\tilde{A}^{(k+1)}_{\mathrm{MA},\nu,k}(Q^2)$: The Form Is Convenient for $Q^2 \sim \Lambda^2_k$.

The results (26) for analytic couplant $\tilde{A}^{(k+1)}_{\mathrm{MA},\nu,k}(Q^2)$ is very convenient at the range at large and at small Q^2 values. For $Q^2 \sim \Lambda^2_i$ the both parts, the standard strong couplant and the additional term, have singularities, which are cancelled in its sum. So, some numerical applications of the results (26) can be complicated. So, here we present another form, which is very useful at $Q^2 \sim \Lambda^2_i$ and can be used also for any Q^2 values, excepting the ranges of very large and very small Q^2 values. As in the previous section, we will present firstly LO results taken from [7] and later to extend them beyond LO.

6.1. LO

The LO minimal analytic coupling $A^{(1)}_{\mathrm{MA},\nu}(Q^2)$ [5,6] have also the another form [7]

$$A^{(1)}_{\mathrm{MA},\nu}(Q^2) = \frac{(-1)}{\Gamma(\nu)} \sum_{r=0}^{\infty} \zeta(1-\nu-r)\, \frac{(-L)^r}{r!} \quad (L < 2\pi), \tag{41}$$

where Euler functions $\zeta(\nu)$ are

$$\zeta(\nu) = \sum_{m=1}^{\infty} \frac{1}{m^{\nu}} = \mathrm{Li}_{\nu}(z=1) \tag{42}$$

The result (41) has been obtained in Ref. [7] considering the property of the Lerch function, which can be considered as a generalization of Polylogarithms (16). The form (41) is very convenient at low L values, t.e. at $Q^2 \sim \Lambda^2$. Moreover, we can use the relation between $\zeta(1-\nu-r)$ and $\zeta(\nu+r)$ functions

$$\zeta(1-\nu-r) = \frac{2\Gamma(\nu+r)}{(2\pi)^{\nu+r}}\, Sin\Big[\frac{\pi}{2}(1-\nu-r)\Big]\, \zeta(\nu+r) \tag{43}$$

For $\nu = 1$ we have

$$A^{(1)}_{\mathrm{MA}}(L) = -\sum_{r=0}^{\infty} \zeta(-r)\, \frac{(-L)^r}{r!} \tag{44}$$

with

$$\zeta(-r) = (-1)^r\, \frac{B_{r+1}}{r+1} \tag{45}$$

and B_{r+1} are Bernoulli numbers.

Using the properties of Bernoulli numbers (δ^0_m is Kronecker symbol), we have for even $r = 2m$ and for odd $r = 1 + 2l$ values

$$\zeta(-2m) = -\frac{\delta^0_m}{2}, \;\; \zeta(-(1+2l)) = -\frac{B_{2(l+1)}}{2(l+1)}\,. \tag{46}$$

Thus, we have for $A^{(1)}_{\mathrm{MA}}(Q^2)$ the following results

$$A^{(1)}_{\mathrm{MA}}(Q^2) = \frac{1}{2}\left(1 + \sum_{l=0}^{\infty} \frac{B_{2(l+1)}}{l+1}\, \frac{(-L)^{2l+1}}{(2l+1)!}\right) = \frac{1}{2}\left(1 + \sum_{s=1}^{\infty} \frac{B_{2s}}{s}\, \frac{(-L)^{2s-1}}{(2s-1)!}\right), \tag{47}$$

with $s = l + 1$.

6.2. Beyond LO

Now we consider the derivatives of (minimal) analytic couplants $\tilde{A}^{(1)}_{\mathrm{MA},\nu}$, shown in Eq.(20), as in Eq. (26), i.e.

$$\tilde{A}^{(i+1)}_{\mathrm{MA},\nu,i}(Q^2) = \tilde{A}^{(1)}_{\mathrm{MA},\nu,i}(Q^2) + \sum_{m=1}^{i} C^{\nu+m}_{m}\, \tilde{\delta}^{(m+1)}_{\mathrm{MA},\nu,i}(Q^2) \tag{48}$$

 doi:10.20944/preprints202412.1263.v1

where $\tilde{A}^{(1)}_{\mathrm{MA},\nu,i} = A^{(1)}_{\mathrm{MA},\nu}$ is given above in (41) with $L \to L_i$ and

$$\tilde{\delta}^{(m+1)}_{\mathrm{MA},\nu,i}(Q^2) = \hat{R}_m\, A^{(1)}_{\mathrm{MA},\nu+m,i}\,, \tag{49}$$

where operators $\hat{R}_m$ are given above in (14).

After come calculations we have

$$\tilde{\delta}^{(m+1)}_{\mathrm{MA},\nu,k}(Q^2) = \frac{(-1)}{\Gamma(\nu+m)} \sum_{r=0}^{\infty} \tilde{R}_m(\nu+r)\, \frac{(-L_k)^r}{r!} \tag{50}$$

where (in an agreement with (34))

$$\begin{aligned}
\tilde{R}_1(\nu+r) &= b_1\Big[\overline{\gamma}_{\mathrm{E}}\zeta(-\nu-r) + \zeta_1(-\nu-r)\Big],\\
\tilde{R}_2(\nu+r) &= b_2\zeta(-\nu-r-1) + b_1^2\Big[\zeta_2(-\nu-r-1) + 2\overline{\gamma}_{\mathrm{E}}\zeta_1(-\nu-r-1)\\
&\quad + \big[\overline{\gamma}_{\mathrm{E}}^2 - \zeta_2\big]\zeta(-\nu-r-1)\Big],
\end{aligned} \tag{51}$$

and

$$\zeta_n(\nu) = \mathrm{Li}_{\nu,n}(z=1) = \sum_{m=1}^{\infty} \frac{\ln^n m}{m^{\nu}}\,. \tag{52}$$

Strictly speaking, the series representation (52) for the functions $\zeta_n(-m-\nu-r-k)$ is not a good definition for large r values and we can replace them by $\zeta_n(m+\nu+r+k)$ using the result (43). However, the results are long and presented in Appendix B.

6.3. The Case $\nu = 1$

For the case $\nu = 1$ we immediately have

$$A^{(i+1)}_{\mathrm{MA,i}}(Q^2) = A^{(1)}_{\mathrm{MA,i}}(Q^2) + \sum_{m=1}^{i} \tilde{\delta}^{(m+1)}_{\mathrm{MA,^\circ=1,i}}(Q^2)\,, \tag{53}$$

$$\delta^{(m+1)}_{\mathrm{MA,i}}(L) \equiv \tilde{\delta}^{(m+1)}_{\mathrm{MA,^\circ=1,i}}(Q^2) = \frac{(-1)}{m!} \sum_{r=0}^{\infty} \tilde{R}_m(1+r)\, \frac{(-L_i)^r}{r!}\,, \tag{54}$$

where $A^{(1)}_{\mathrm{MA,i}}(Q^2)$ is given above in (44) (with the replacement $(L \to L_i)$ and the coefficients $\tilde{R}_m(1+r)$ can be found in (51) when $\nu = 1$.

The results (54) can be expressed in terms of the functions $\zeta_n(m+\nu+r+k)$. Using the results in Appendix D and taking the even part ($r = 2m$) and the odd part ($r = 2s-1$) (see equation (B2)), we have

$$\begin{aligned}
\delta^{(2)}_{\mathrm{MA},k}(Q^2) &= \frac{2}{(2\pi)^2}\left[\sum_{m=0}^{\infty}(2m+1)(-1)^m Q_{1a}(2m+2)\hat{L}_k^{2m} - \pi\sum_{s=1}^{\infty} s(-1)^s Q_{1b}(2s+1)\hat{L}_k^{2s-1}\right],\\
\delta^{(3)}_{\mathrm{MA},k}(Q^2) &= -\frac{1}{(2\pi)^3}\left[\pi\sum_{m=0}^{\infty}(2m+1)(m+1)(-1)^m Q_{2b}(2m+3)\hat{L}_k^{2m}\right.\\
&\quad \left. +2\sum_{s=1}^{\infty} s(2s+1)(-1)^s Q_{2a}(2s+2)\hat{L}_k^{2s-1}\right],
\end{aligned} \tag{55}$$

where

$$\hat{L}_k = \frac{L_k}{2\pi} \tag{56}$$

and the function Q_{ma} and Q_{mb} are given in Appendix B.

 doi:10.20944/preprints202412.1263.v1

At the point $L_k = 0$, i.e. $Q^2 = \Lambda_k^2$, we have

$$A_{\rm MA}^{(1)} = \frac{1}{2}, \quad \delta_s^{(2)} = \frac{2}{(2\pi)^2} Q_{1a}(2) = -\frac{b_1}{2\pi^2}\Big(\zeta_1(2) + l\zeta(2)\Big),$$
$$\delta_s^{(3)} = -\frac{\pi}{(2\pi)^3} Q_{2b}(3) = \frac{b_1^2}{4\pi^2}\Big(\zeta_1(3) + (2l-1)\zeta(3)\Big), \tag{57}$$

where $\zeta_k(\nu)$ are given in Eq. (52) and

$$l = \ln(2\pi)\,. \tag{58}$$

7. Integral Representations for $\tilde{A}^{(i)}_{\rm MA,\,\circ}(Q^2)$

As already discussed in Introduction, the MA couplant $A^{(1)}_{\rm MA}(Q^2)$ is constructed as follows: the LO spectral function is taken directly from perturbation theory but the MA couplant $A^{(1)}_{\rm MA}(Q^2)$ itself was built using the correct integration counter. Thus, at LO, the MA couplant $A^{(1)}_{\rm MA}(Q^2)$ obeys Eq. (5) presented in Introduction.

For the ν-derivative of $A^{(1)}_{\rm MA}(Q^2)$, i.e. $\tilde{A}^{(1)}_{\rm MA,\,\circ}(Q^2)$, there is the following equation [34]:

$$\tilde{A}^{(1)}_{\rm MA,\,\circ}(Q^2) = \frac{(-1)}{\Gamma(\nu)}\int_0^\infty \frac{ds}{s} r_{\rm pt}^{(1)}(s){\rm Li}_{1-\nu}(-sz)\,, \tag{59}$$

where $r_{\rm pt}^{(1)}(s)$ is the LO spectral function defined in Eq. (5) and ${\rm Li}_{1-\nu}(-sz)$ is the Polylogarithmic function presented in (16).

Beyond LO, Eq. (59) can be extended in two ways, which will be shown in following subsections.

7.1. Modification of Spectral Functions

The first possibility to extend the result (59) beyond LO is related to the modification of the spectral function. The extension is simple and the final result looks like this:

$$\tilde{A}^{(i+1)}_{{\rm MA},\nu,k}(Q^2) = \frac{(-1)}{\Gamma(\nu)}\int_0^\infty \frac{ds}{s} r_{\rm pt}^{(i+1)}(s){\rm Li}_{1-\nu}(-sz_k)\,, \tag{60}$$

i.e. it is similar to (59) with the replacement the LO spectral function $r_{\rm pt}^{(1)}(s)$ by $i+1$-order one $r_{\rm pt}^{(i+1)}(s)$:

$$r_{\rm pt}^{(i+1)}(s) = r_{\rm pt}^{(1)}(s) + \sum_{m=1}^{i}\delta_{\rm r}^{(m+1)}(s) \tag{61}$$

and (see [17])

$$y = \ln s, \quad r_{\rm pt}^{(1)}(y) = \frac{1}{y^2+\pi^2}\,, \quad \delta_{\rm r}^{(2)}(y) = -\frac{b_1}{(y^2+\pi^2)^2}\Big[2yf_1(y) + (\pi^2-y^2)f_2(y)\Big]\,, \tag{62}$$

with

$$f_1(y) = \frac{1}{2}\ln(y^2+\pi^2), \quad f_2(y) = \frac{1}{2} - \frac{1}{\pi}arctan\Big(\frac{y}{\pi}\Big)\,. \tag{63}$$

For the couplant itself, we have

$$A^{(i+1)}_{\rm MA,k}(Q^2) \equiv \tilde{A}^{(i+1)}_{{\rm MA},\nu=1,k}(Q^2) = \int_0^{+\infty}\frac{ds\, r_{\rm pt}^{(i+1)}(s)}{(s+t_k)}\,. \tag{64}$$

Numerical evaluations of the integrals in (64) can be done following to discussions in Section 4 in Ref. [36].

 doi:10.20944/preprints202412.1263.v1

7.2. Modification of Polylogaritms

Beyond LO, the results (59) can be extended also by using the $\hat{R}_m$ operators shown in (14). This is the path already used in Sections 4 and 5 to obtain other $\tilde{A}^{(i+1)}_{\text{MA},\nu,i}(Q^2)$ results.

Here, the application of the operators $\hat{R}_m$ for Eq. (59) leads to the following result:

$$\tilde{A}^{(i+1)}_{\text{MA},\nu,i}(Q^2) = \int_0^\infty \frac{ds}{s} r^{(1)}_{\text{pt}}(s) \tilde{\Delta}^{(i+1)}_{\nu,i}\,, \tag{65}$$

where the results for $\tilde{\Delta}^{(i+1)}_{\nu,i}$ can be found in Eqs. (23) and (24) and also in Eq. (34).

For MA couplant itself, we have beyond LO

$$A^{(i+1)}_{\text{ma,i}}(Q^2) \equiv \tilde{A}^{(i+1)}_{\text{ma},\nu=1,i}(Q^2) = \int_0^{+\infty} \frac{ds}{s} r^{(1)}_{\text{pt}}(s) \tilde{\Delta}^{(i+1)}_{\nu=1,i}\,, \tag{66}$$

where the results for $\tilde{\Delta}^{(i+1)}_{\nu=1,i}$ are given in Eqs. (23) and (24) with $\nu = 1$, i.e.

$$\tilde{\Delta}^{(i+1)}_{\nu=1,i} = \tilde{\Delta}^{(1)}_{1,i} + \sum_{m=1}^{i} \frac{P_{m,1}(z_i)}{m!} = \Delta^{(1)}_{1,i} + \sum_{m=1}^{i} \frac{P_{m,1}(z_i)}{m!}\,, \tag{67}$$

where $\Delta^{(1)}_{1,i} = \text{Li}_0(z_i)$ and $P_{m,1}(z_i)$ are given in Eq. (34).

7.3. Discussions

We have considered $1/L$-expansions of ν-derivatives of the strong couplant a_s expressed as combinations of operators $\hat{R}_m$ (14) applied to the LO couplant $a_s^{(1)}$. Applying the same operators to the ν-derivatives of the LO MA couplant $A^{(1)}_{\text{MA}}$, we obtained four different representations for the ν-derivatives of the MA couplants, i.e. $\tilde{A}^{(i)}_{\text{MA},\,\circ}$, in each i-order of perturbation theory: one form contains a combination of Polylogarithms; the other contains an expansion of the generalized Euler ζ-function, and the third is based on dispersion integrals containing the LO spectral function. We also obtained a fourth representation based on the dispersion integral containing the i-order spectral function. All results are presented up to the 5th order of perturbation theory, where the corresponding coefficients of the QCD β-function are well known (see [2,3]).

The high-order corrections are negligible in the $Q^2 \to 0$ and $Q^2 \to \infty$ asymptotics and are nonzero in the vicinity of the point $Q^2 = \Lambda^2$. Thus, in fact, they are really only small corrections to the LO MA couplant $A^{(1)}_{\text{MA},\,\circ}(Q^2)$. This proves the possibility of expansions of high-order couplants $A^{(i)}_{\text{MA},\,\circ}(Q^2)$ via the LO couplants $A^{(1)}_{\text{MA},\,\circ}(Q^2)$, which was done in Ref. [9], as well as the possibility of various approximations used in [28,38–40].

8. Integral Representations for $\tilde{U}^{(i)}_{\text{MA},\,\circ}(s)$

As it was abovementioned in Introduction, the MA couplants $A^{(1)}_{\text{MA},\,\circ}(Q^2)$ and $U^{(1)}_{\text{MA},\,\circ}(s)$ are constructed as follows: the LO spectral function is taken directly from perturbation theory but the MA couplants $A^{(1)}_{\text{MA},\,\circ}(Q^2)$ and $U^{(1)}_{\text{MA},\,\circ}(s)$ themselves were obtained using the correct integration contours. Thus, at LO, the MA couplants $A^{(1)}_{\text{MA},\,\circ}(Q^2)$ and $U^{(1)}_{\text{MA},\,\circ}(s)$ obey Eqs. (5) and (6) presented in Introduction.

To check Eqs. (29) and (30) we compare them with an integral form

$$U^{(i)}_1(\text{s}) = \frac{1}{\pi} \int_s^\infty \frac{d\sigma}{\sigma} r^{(i)}_{\text{pt}}(\sigma). \tag{68}$$

 doi:10.20944/preprints202412.1263.v1

For LO, we can take the integral form from [8]

$$U_\nu^{(1)}(\mathrm{s}) = \frac{1}{\pi}\int\limits_s^\infty \frac{d\sigma}{\sigma} r_\nu^{(1)}(\sigma), \tag{69}$$

where

$$r_\nu^{(1)}(\mathrm{s}) = \frac{\sin[\nu\, g(s)]}{\pi(\pi^2+L_s^2)^{(\nu-1)/2}} = \nu\, U_{\nu+1}^{(1)}(\mathrm{s})\,, \tag{70}$$

Using our approach to obtain high-order terms from LO (69), we can extend the LO integral (69) to the one

$$\tilde{U}_\nu^{(i)}(\mathrm{s}) = \frac{1}{\pi}\int\limits_s^\infty \frac{d\sigma}{\sigma} r_\nu^{(i)}(\sigma), \tag{71}$$

where obviously

$$r_\nu^{(i)}(\mathrm{s}) = \nu\, \tilde{U}_{\nu+1}^{(i)}(\mathrm{s})\,. \tag{72}$$

The spectral function $r_1^{(i)}(\mathrm{s})$ has the form

$$r_1^{(i)}(\mathrm{s}) = r_1^{(1)}(\mathrm{s}) + \sum_{m=1}^{i} \delta_1^{(m+1)}(\mathrm{s}) \tag{73}$$

where

$$r_1^{(1)}(\mathrm{s}) = U_2^{(1)}(\mathrm{s}),\;\; \delta_1^{(m+1)}(\mathrm{s}) = (m+1)\,\tilde{\delta}_{\nu=2}^{(m+1)}(\mathrm{s}). \tag{74}$$

In the explicit form:

$$\begin{aligned} r_1^{(i)}(\mathrm{s}) &= \frac{\sin(g)}{\pi(\pi^2+L_s^2)^{1/2}} = \frac{1}{\pi^2+L_s^2}, \\ \tilde{\delta}_1^{(m+1)}(\mathrm{s}) &= \frac{1}{\pi(\pi^2+L_s^2)^{(m+1)/2}}\Big\{\overline{\delta}_m^{(m+1)}(\mathrm{s})\sin\big((m+1)g\big) + \hat{\delta}_m^{(m+1)}(\mathrm{s})g\cos\big((m+1)g\big)\Big\}, \end{aligned} \tag{75}$$

where $\overline{\delta}_m^{(m+1)}(\mathrm{s})$ and $\hat{\delta}_m^{(m+1)}(\mathrm{s})$ can be obtained from the results in (30) with $\nu = 2$. They are

$$\begin{aligned} &\overline{\delta}_1^{(2)}(\mathrm{s}) = -G\,b_1,\;\; \hat{\delta}_1^{(2)}(\mathrm{s}) = b_1\,, \\ &\overline{\delta}_2^{(3)}(\mathrm{s}) = b_2 + b_1^2\Big[G^2 - g^2 - G - 1\Big],\;\; \hat{\delta}_2^{(3)}(\mathrm{s}) = b_1^2\Big[1-2G\Big]\,. \end{aligned} \tag{76}$$

Using the results (36) and (37) for $\cos(ng)$ and $\sin(ng)$ $(n \le 4)$, we see that with the results [36,37] (see also Section 6 in [18]) give more compact results for $r_1^{(i)}(\mathrm{s})$. We think that Eqs. (75) and (76) give apparently very compact results for $r_1^{(i)}(\mathrm{s})$.

Note that the results (71) for $\tilde{U}_\nu^{(i)}(\mathrm{s})$ are exactly the same as the results in Eq. (28) done in the form of trigonometric factions. However the results (71) should be very handy in case of non-minimal versions of analytic couplants (see Refs. [30,31,33]).

9. $H \to b\bar{b}$ Decay

In Ref. [18] we used the polarized Bjorken sum rule [62] as an example for the application of the MA couplant $A_{\rm MA}(Q^2)$, which is a popular object of study in the framework of analytic QCD (see [38,40,60,61]). Here we consider the decay of the Higgs boson into a bottom-antibottom pair, which is also a popular application of the MA couplant $U_{\rm MA}(Q^2)$ (see, e.g., [8] and reviews in Ref. [16]).

 doi:10.20944/preprints202412.1263.v1

The Higgs-boson decay into a bottom-antibottom pair can be expressed in QCD by means of the correlator

$$\Pi(Q^2) = (4\pi)^2 i \int dx e^{iqx} < 0|T[J_b^S(x) J_b^S(0)]0 > \tag{77}$$

of two quark scalar (S) currents in terms of the discontinuity of its imaginary part, i.e., $R_S(s) = \mathbf{Im}\Pi(-s - i\varepsilon)/(2\pi s)$, so that the width reads

$$\Gamma(H \to b\bar{b}) = \frac{G_F}{4\sqrt{2}\pi} M_H m_b^2(M_H^2) R_s(s = M_H^2)\,. \tag{78}$$

Direct multi-loop calculations were performed in the Euclidean (spacelike) domain for the corresponding Adler function D_S (see Refs. [41–44]). Hence, we write ($D_s \to \tilde{D}_s$ and $R_s \to \tilde{R}_s$ because the additional factor m_b^2)

$$\tilde{D}(Q^2) = 3m_b^2(Q^2)\Big[1 + \sum_{n\geq 1} d_n\, a_s^n(Q^2)\Big], \tag{79}$$

where for $f = 5$ the coefficients d_n are

$$d_1 = 2.96,\;\; d_2 = 11.44,\;\; d_2 = 50.17,\;\; d_4 = 260.24, \tag{80}$$

Taking the imagine part, one has

$$\tilde{R}_s(s) = 3m_b^2(s)\Big[1 + \sum_{n\geq 1} r_n\, a^n(s)\Big], \tag{81}$$

and for $f = 5$ [43,45]

$$r_1 = 2.96,\;\; r_2 = 7.93,\;\; r_3 = 5.93,\;\; r_4 = -61.84, \tag{82}$$

Here $\overline{m}_b^2(Q^2)$ has the form (see Appendix C):

$$\overline{m}_b^2(Q^2) = \hat{m}_b^2 a_s^d(Q^2)\left[1 + \sum_{k=1}^{k=4} \bar{e}_k\, a_s^k(Q^2)\right], \tag{83}$$

where

$$\bar{e}_k = \frac{\tilde{e}_k}{k(\beta_0)^k} \tag{84}$$

and $\tilde{e}_k$ are done in Eq. (C8). For $f = 5$ we have

$$\bar{e}_1 = 1.23,\;\; \bar{e}_2 = 1.20,\;\; \bar{e}_3 = 0.55,\;\; \bar{e}_4 = 0.54\,. \tag{85}$$

The normalization constant $\hat{m}_b$ cab be obtained as (see, e.g., [16])

$$\hat{m}_b = \overline{m}_b(Q^2 = m_b^2) a_s^{-d/2}(m_b^2)\left[1 + \sum_{k=1}^{k=4} \bar{e}_k\, a_s^k(Q^2)\right]^{-1/2} = 10.814\ \mathrm{GeV}^2\,, \tag{86}$$

since $\overline{m}_b(Q^2 = m_b^2) = m_b = 4.18$ GeV.

So, we have

$$\tilde{R}_s(s) = \tilde{R}_s^{(m=5)}(s),\;\; \tilde{R}_s^{(m+1)}(s) = 3\hat{m}_b^2\, a_s^d(s)\left[1 + \sum_{k=0}^{m} \bar{r}_k a_s^k(s))\right], \tag{87}$$

where

$$\bar{r}_k = r_k + \bar{e}_k + \sum_{l=1}^{k-1} r_l\, \bar{e}_{k-l}\,. \tag{88}$$

 doi:10.20944/preprints202412.1263.v1

For $f = 5$ we have

$$\bar{r}_1 = 4.18,\ \ \bar{r}_2 = 12.76,\ \ \bar{r}_3 = 19.76,\ \ \bar{r}_4 = -42.25\,. \tag{89}$$

We can express all results through derivatives $\tilde{a}_{d+k}$ (see Appendix A):

$$\tilde{R}_s(s) = \tilde{R}_s^{(m=5)}(s),\ \ \tilde{R}_s^{(m+1)}(s) = 3\hat{m}_b^2\left[\tilde{a}_d + \sum_{k=0}^{m} \tilde{r}_k \tilde{a}_{d+k}\right], \tag{90}$$

where

$$\tilde{r}_k = \bar{r}_k + \tilde{k}_k(d) + \sum_{l=1}^{k-1} \bar{r}_l\, \tilde{k}_{k-l}(d+l)\,, \tag{91}$$

where $\tilde{k}_i(\nu)$ are given in Appendix A.

For $d = 24/23$ and $f = 5$, we have

$$\tilde{r}_1 = 4.17,\ \ \tilde{r}_2 = 9.86,\ \ \tilde{r}_3 = 1.29,\ \ \tilde{r}_4 = -71.21\,. \tag{92}$$

Performing the same analysis for the Adler function we have

$$\tilde{D}_s = \tilde{D}_s^{(m=5)},\ \ \tilde{D}_s^{(m+1)} = 3\hat{m}_b^2 a_s^d(Q^2)\left[1 + \sum_{k=0}^{m} \bar{d}_k a_s^k(Q^2))\right], \tag{93}$$

where

$$\bar{d}_k = r_k + \bar{e}_k + \sum_{l=1}^{k-1} d_l\, \bar{e}_{k-l}\,. \tag{94}$$

For $f = 5$ we have

$$\bar{d}_1 = 4.18,\ \ \bar{d}_2 = 16.27,\ \ \bar{d}_3 = 68.30,\ \ \bar{r}_4 = 337.66\,. \tag{95}$$

We express all results through derivatives $\tilde{a}_{d+k}$:

$$\tilde{D}_s = \tilde{D}_s^{(m=5)},\ \ \tilde{D}_s^{(m+1)} = 3\hat{m}_b^2\left[\tilde{a}_d(Q^2) + \sum_{k=0}^{m} \tilde{d}_k \tilde{a}_{d+k}(Q^2)\right], \tag{96}$$

where

$$\tilde{d}_k = \bar{d}_k + \tilde{k}_k(d) + \sum_{l=1}^{k-1} \bar{d}_l\, \tilde{k}_{k-l}(d+l)\,. \tag{97}$$

For $f = 5$ and $d = 24/23$, we have

$$\tilde{d}_1 = 4.17,\ \ \tilde{d}_2 = 13.37,\ \ \tilde{d}_3 = 43.90,\ \ \tilde{d}_4 = 178.18\,. \tag{98}$$

As it was discussed earlier in [8] in FAPT there are the following representation for $\tilde{R}_s$

$$\tilde{R}_s(s) = \tilde{R}_s^{(m=5)}(s),\ \ \tilde{R}_s^{(m+1)}(s) = 3\hat{m}_b^2\left[\tilde{U}_d^{(m+1)}(\mathrm{s}) + \sum_{k=0}^{m} \tilde{d}_k\, \tilde{U}_{d+k}^{(m+1)}(s)\right], \tag{99}$$

The results for $\tilde{R}_s^{(m+1)}(s)$ are shown in Figure 14. We see that the FAPT results (99) are lower than those (90) based on the conventional PT. This is in full agreement with arguments given in [16]. But the difference becomes less notable as the PT order increases. Indeed, for N^{3}LO the difference is very small, which proves the assumption about the possibility of using $\tilde{R}_s^{(m+1)}(s)$ expression for $\tilde{D}_s^{(m+1)}(Q^2)$ with $A_{\rm MA}^{(i)}(Q^2) \to U_{\rm MA}^{(i)}(s)$, which was done in Ref. [8].

Preprints.org (www.preprints.org) | NOT PEER-REVIEWED | Posted: 16 December 2024 doi:10.20944/preprints202412.1263.v1

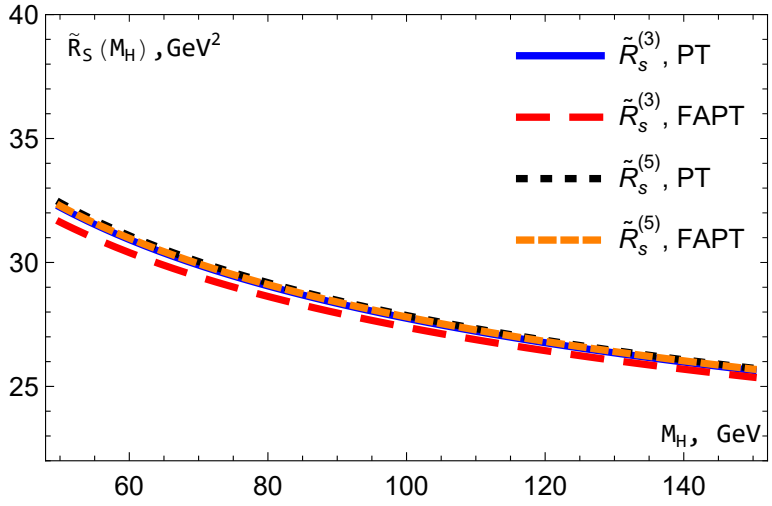

Figure 14. The results for $\tilde{R}_s^{(m+1)}(s)$ with $m = 2$ and 4 in the framework of the usual PT and FAPT.

The results for $\Gamma^{(m)}(H \to b\bar{b})$ in the N^{m}LO approximation using $\tilde{R}_s^{(m+1)}(s)$ from Eqs. (87) and (90) are exactly same and have the following form:

$$\Gamma^{(0)} = 1.76\,\text{MeV},\ \Gamma^{(1)} = 2.27\,\text{MeV},\ \Gamma^{(2)} = 2.37\,\text{MeV},$$
$$\Gamma^{(3)} = 2.38\,\text{MeV},\ \Gamma^{(4)} = 2.38\,\text{MeV}. \tag{100}$$

The corresponding results for $\Gamma^{(m)}(H \to b\bar{b})$ with $\tilde{R}_s^{(m+1)}(s)$ form Eq. (99) are very similar to ones in (100). They are:

$$\Gamma^{(0)} = 1.74\,\text{MeV},\ \Gamma^{(1)} = 2.23\,\text{MeV},\ \Gamma^{(2)} = 2.34\,\text{MeV},$$
$$\Gamma^{(3)} = 2.37\,\text{MeV},\ \Gamma^{(4)} = 2.38\,\text{MeV}. \tag{101}$$

So, we see a good agreement between the results obtained in FAPT and in the framework of the usual PT.

It is clearly seen that the results of FAPT are very also close to the results [46] obtained in the framework of the now very popular Principle of Maximum Conformality [47] (for the recent review, see [48]). Indeed, our results are within the band obtained by varying the renormalization scale.

The Standard Model expectation is [49]

$$\Gamma^{SM}_{H\to b\bar{b}}(M_H = 125.1\text{GeV}) = 2.38\text{MeV}. \tag{102}$$

The ratios of the measured events yield to the Standard Model expectations are $1.01 \pm 0.12(\text{stat.}) + 0.16 - 0.15(\text{syst.})$ [50] in ATLAS Collaboration and $1.04 \pm 0.14(\text{stat.}) \pm 0.14(\text{syst.})$ [51] in SMC Collaboration (see also [52]).

Thus, our results obtained in both approaches, in the standard perturbation theory and in analytical QCD, are in good agreement both with the Standard Model expectations [49] and with the experimental data [50,51].

10. Bjorken Sum Rule

The polarized BSR [53] (see also [54,55]) is defined as the difference between the proton and neutron polarized SFs, integrated over the entire interval x

$$\Gamma_1^{p-n}(Q^2) = \int_0^1 dx\,[g_1^p(x,Q^2) - g_1^n(x,Q^2)]. \tag{103}$$

 doi:10.20944/preprints202412.1263.v1

Theoretically, the quantity can be written in the OPE form (see Ref. [56,57])

$$\Gamma_1^{p-n}(Q^2) = \frac{g_A}{6}\left(1 - D_{\rm BS}(Q^2)\right) + \sum_{i=2}^{\infty} \frac{\mu_{2i}(Q^2)}{Q^{2i-2}}\,, \tag{104}$$

where g_A=1.2762 $\pm$ 0.0005 [24] is the nucleon axial charge, $(1 - D_{BS}(Q^2))$ is the leading-twist (or twist-two) contribution, and μ_{2i}/Q^{2i-2} $(i \geq 1)$ are the higher-twist (HT) contributions.[9]

Since we plan to consider in particular very small Q^2 values here, the representation (104) of the HT a number of infinite terms. To avoid that, it is preferable to use the so-called "massive" twist-four representation, which includes a part of the HT contributions of (104) (see Refs. [58,59]): [10]

$$\Gamma_1^{p-n}(Q^2) = \frac{g_A}{6}\left(1 - D_{\rm BS}(Q^2)\right) + \frac{\hat{\mu}_4 M^2}{Q^2 + M^2}\,, \tag{105}$$

where the values of $\hat{\mu}_4$ and M^2 have been fitted in Refs. [60,61] in the different analytic QCD models.

In the case of MA QCD, from [61] one can see that in (105)

$$M^2 = 0.439 \pm 0.012 \pm 0.463 \;\; \hat{\mu}_{\rm MA,4} = -0.173 \pm 0.002 \pm 0.666\,, \tag{106}$$

where the statistical (small) and systematic (large) uncertainties are presented.

Up to the k-th PT order, the twist-two part has the form

$$D_{\rm BS}^{(1)}(Q^2) = \frac{4}{\beta_0}\, a_s^{(1)}, \;\; D_{\rm BS}^{(k\geq 2)}(Q^2) = \frac{4}{\beta_0}\, a_s^{(k)} \left(1 + \sum_{m=1}^{k-1} d_m \left(a_s^{(k)}\right)^m\right), \tag{107}$$

where d_1, d_2 and d_3 are known from exact calculations (see, for example, [62]). The exact d_4 value is not known, but it was estimated in Ref. [63].

Converting the couplant powers into its derivatives, we have

$$D_{\rm BS}^{(1)}(Q^2) = \frac{4}{\beta_0}\, \tilde{a}_1^{(1)}, \;\; D_{\rm BS}^{(k\geq 2)}(Q^2) = \frac{4}{\beta_0} \left(\tilde{a}_1^{(k)} + \sum_{m=2}^{k} \tilde{d}_{m-1} \tilde{a}_m^{(k)}\right), \tag{108}$$

where

$$\begin{aligned} &\tilde{d}_1 = d_1, \;\; \tilde{d}_2 = d_2 - b_1 d_1, \;\; \tilde{d}_3 = d_3 - \frac{5}{2} b_1 d_2 - \left(b_2 - \frac{5}{2} b_1^2\right) d_1, \\ &\tilde{d}_4 = d_4 - \frac{13}{3} b_1 d_3 - \left(3 b_2 - \frac{28}{3} b_1^2\right) d_2 - \left(b_3 - \frac{22}{3} b_1 b_2 + \frac{28}{3} b_1^3\right) d_1 \end{aligned} \tag{109}$$

and $b_i = \beta_i/\beta_0^{i+1}$.

In MA QCD, the results (105) become as follows (some analyses based on other approaches can be found in [64–66])

$$\Gamma_{\rm MA,1}^{p-n}(Q^2) = \frac{g_A}{6}\left(1 - D_{\rm MA,BS}(Q^2)\right) + \frac{\hat{\mu}_{\rm MA,4} M^2}{Q^2 + M^2}, \;\; , \tag{110}$$

---

[9] Below, in our analysis, the so-called elastic contribution will always be excluded.

[10] Note that Ref. [59] also contains a more complicated form for the "massive" twist-four part. It was included in our previous analysis in [21], but will not be considered here.

 doi:10.20944/preprints202412.1263.v1

where the perturbative part $D_{\rm BS,MA}(Q^2)$ takes the same form, however, with analytic couplant $\tilde{A}^{(k)}_{\rm MA,\,^\circ}$ (the corresponding expressions are taken from [18])

$$D^{(1)}_{\rm MA,BS}(Q^2) = \frac{4}{\beta_0}\, A^{(1)}_{\rm MA}, \;\; D^{k\geq 2}_{\rm MA,BS}(Q^2) = \frac{4}{\beta_0}\left(A^{(1)}_{\rm MA} + \sum_{m=2}^{k} \tilde{d}_{m-1}\, \tilde{A}^{(k)}_{\rm MA,\,^\circ=m}\right). \tag{111}$$

We would like to note the coefficients β_i depend on the number f of active quarks, which changes at thresholds $Q^2_f \sim m^2_f$, where some additional quark comes to play at $Q^2 > Q^2_f$. Here m_f is the $\overline{MS}$ mass of f quark. So, the coupling constant a_s is f-dependent and the f-dependence can be taken into the corresponding QCD parameter Λ. , i.e. Λ^f contribute to above Eqs. (107), (108) and (111).

The relations between Λ^f_i and Λ^{f-1}_i are coming from the decoupling relations, i.e. the relations between $a_s(f, Q^2_f)$ and $a_s(f-1, Q^2_f)$. In the $\overline{MS}$ scheme, the decoupling relations are known up to four-loop order [25] and they are usually used at $Q^2_f = m^2_f$, where the relations are simplified (for a recent review, see e.g. [67]).

Here we will not consider the f-dependence of Λ^f_i and $a_s(f, M^2_Z)$. Since we will mainly consider the region of low Q^2, we will use the results for $\Lambda^{f=3}_i$, which we need to construct the analytic couplant for small Q^2 values.

For the k-th order of PT, we use the results (11) for $\Lambda^{f=3}_{k-1}$ $(k = 1, 2, 3, 4)$ taken from the recent Ref. [27], which corresponds to the middle value of the world average $\alpha_s(M^2_z) = 0.1179 \pm 0.0009$ [24]. We use also $\Lambda_4 = \Lambda_3$, since in highest orders Λ_i values become very similar. Moreover, since the results for $\alpha_s(M^2_z)$ and for $\Lambda^{f=3}_{k-1}$ are taken from the range of Q^2 values where the difference between the analytic and usual couplants is small, we use the values (11) also in the case of anaytic QCD.

For the case of 3 active quark flavors ($f = 3$), which is accepted in this paper, we have

$$\begin{aligned} &d_1 = 1.59, \;\; d_2 = 3.99, \;\; d_3 = 15.42 \;\; d_4 = 63.76, \\ &\tilde{d}_1 = 1.59, \;\; \tilde{d}_2 = 2.73, \;\; \tilde{d}_3 = 8.61, \;\; \tilde{d}_4 = 21.52\,, \end{aligned} \tag{112}$$

i.e., the coefficients in the series of derivatives are slightly smaller.

10.1. Results

The fitting results of experimental data (see [68–74]) obtained only with statistical uncertainties are presented in Table 1 and shown in Figures 15 and 16. For the fits we use Q^2-independent M^2 and $\hat{\mu}_4$ and the two-twist part shown in Eqs. (108), (111) for regular PT and APT, respectively.

As it can be seen in Figure 15, with the exception of LO, the results obtained using conventional couplant are very poor. Moreover, the discrepancy in this case increases with the order of PT (see also [38,39,60,61] for similar analyses). The LO results describe experimental points relatively well, since the value of $\Lambda_{\rm LO}$ is quite small compared to other Λ_i, and disagreement with the data begins at lower values of Q^2 (see Figure 4 below). Thus, using the "massive" twist-four form (105) does not improve these results, since with $Q^2 \to \Lambda^2_i$ conventional couplants become singular, which leads to large and negative results for the twist-two part (107). So, as the PT order increases, ordinary couplants become singular for ever larger Q^2 values, while BSR tends to negative values for ever larger Q^2 values.

Preprints.org (www.preprints.org) | NOT PEER-REVIEWED | Posted: 16 December 2024 doi:10.20944/preprints202412.1263.v1

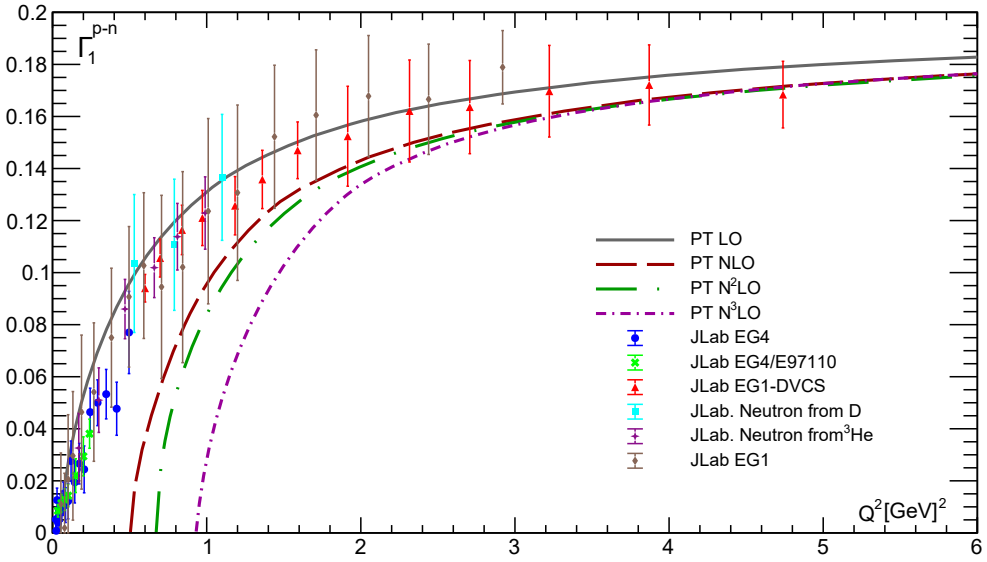

Figure 15. The results for $\Gamma_1^{p-n}(Q^2)$ in the first four orders of PT.

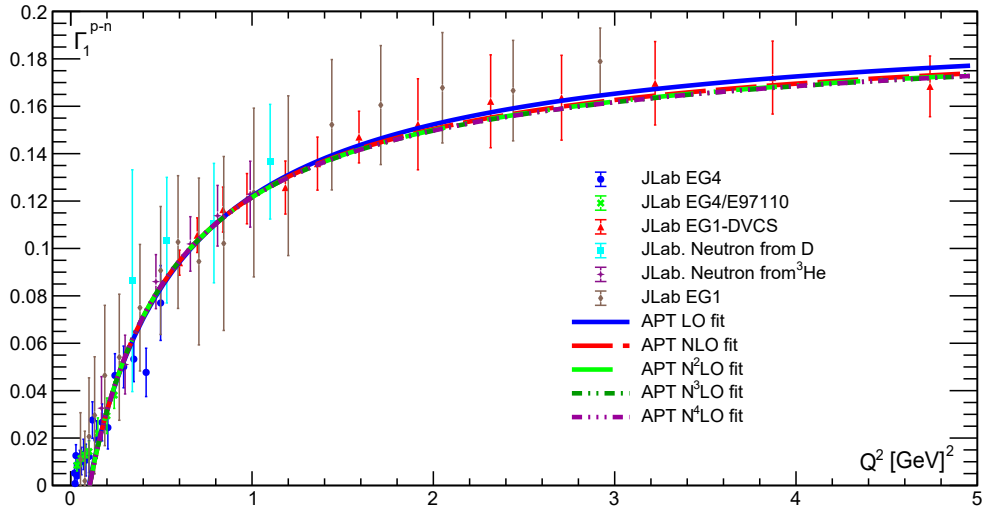

Figure 16. The results for $\Gamma_1^{p-n}(Q^2)$ in the first four orders of APT.

In contrast, our results obtained for different APT orders are practically equivalent: the corresponding curves become indistinguishable when Q^2 approaches 0 and slightly different everywhere else. As can be seen in Figure 16, the fit quality is pretty high, which is demonstrated by the values of the corresponding $\chi^2/(\text{d.o.f.})$ (see Table 1).

 doi:10.20944/preprints202412.1263.v1

Table 1. The values of the fit parameters in (110).

	M^2 [GeV^2] for $Q^2 \leq 5$ GeV^2 (for $Q^2 \leq 0.6$ GeV^2)	$\hat{\mu}_{MA,4}$ for $Q^2 \leq 5$ GeV^2 (for $Q^2 \leq 0.6$ GeV^2)	χ^2/(d.o.f.) for $Q^2 \leq 5$ GeV^2 (for $Q^2 \leq 0.6$ GeV^2)
LO	0.472 ± 0.035 (1.631 ± 0.301)	-0.212 ± 0.006 (-0.166 ± 0.001)	0.667 (0.789)
NLO	0.414 ± 0.035 (1.545 ± 0.287)	-0.206 ± 0.008 (-0.155 ± 0.001)	0.728 (0.757)
N^{2}LO	0.397 ± 0.034 (1.417 ± 0.241)	-0.208± 0.008 (-0.156 ± 0.002)	0.746 (0.728)
N^{3}LO	0.394 ± 0.034 (1.429 ± 0.248)	-0.209 ± 0.008 (-0.157 ± 0.002)	0.754 (0.747)
N^{4}LO	0.397 ± 0.035 (1.462 ± 0.259)	-0.208 ± 0.007 (-0.157 ± 0.001)	0.753 (0.754)

10.2. Low Q^2 Values

The full picture, however, is more complex than shown in Figure 16. The APT fitting curves become negative (see Figure 17) when we move to very low values of Q^2: Q^2 <0.1 GeV^2. So, the good quality of the fits shown in Table 1 was obtained due to good agreement with experimenatl data at Q^2 >0.2 GeV^2. The picture improves significantly when we compare our result with experimental data for Q^2 <0.6 GeV^2 (see Figure 18 and Ref. [21]).

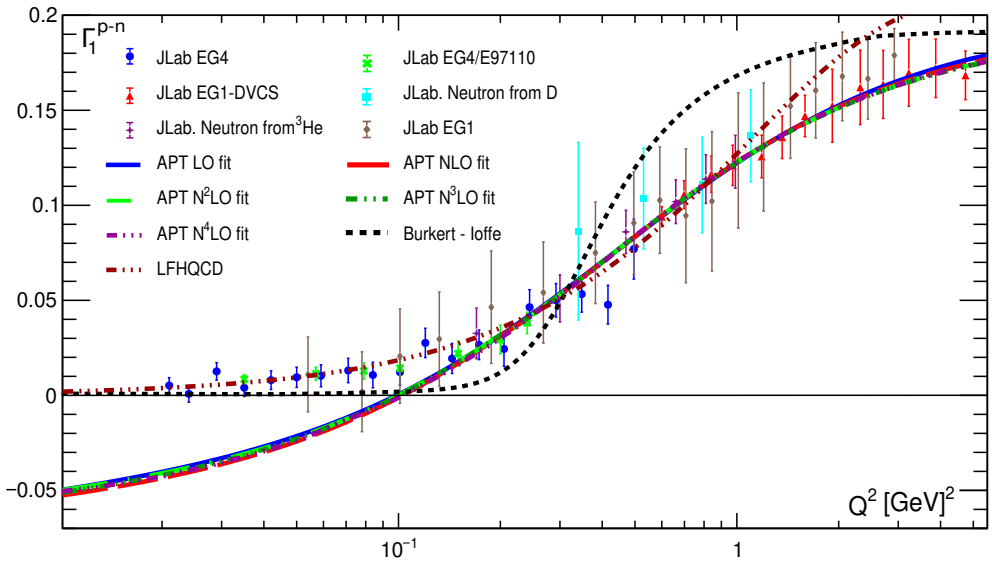

Figure 17. Same as in Figure 16 but for Q^2 <0.6 GeV^2.

Figure 18 also shows contributions from conventional PT in the first two orders: the LO and NLO predictions have nothing in common with experimental data. As we mentioned above, higher orders lead to even worse agreement, and they are not shown. The purple curve emphasizes the key role of the twist-four contribution (see also [39,75]) and the discussions therein). Excluding this contribution, the value of $\Gamma_1^{p-n}(Q^2)$ is about 0.16, which is very far from the experimental data.

At $Q^2 \leq 0.3$GeV^2, we also see the good agreement with the phenomenological models: LFHQCD [76] and the correct IR limit of Burkert–Ioffe model [77].For larger values of Q^2, our results are lower than the results of phenomenological models, and for $Q^2 \geq 0.5$GeV^2 below the experimental data.

Nevertheless, even in this case where very good agreement with experimental data with Q^2 <0.6 GeV^2 is demonstrated, our results for $\Gamma_{MA,1}^{p-n}(Q^2)$ take negative unphysical values when Q^2 <0.02

Preprints.org (www.preprints.org) | NOT PEER-REVIEWED | Posted: 16 December 2024 doi:10.20944/preprints202412.1263.v1

GeV^2. The reason for this phenomenon can be shown by considering photoproduction within APT, which is the topic of the next subsection.

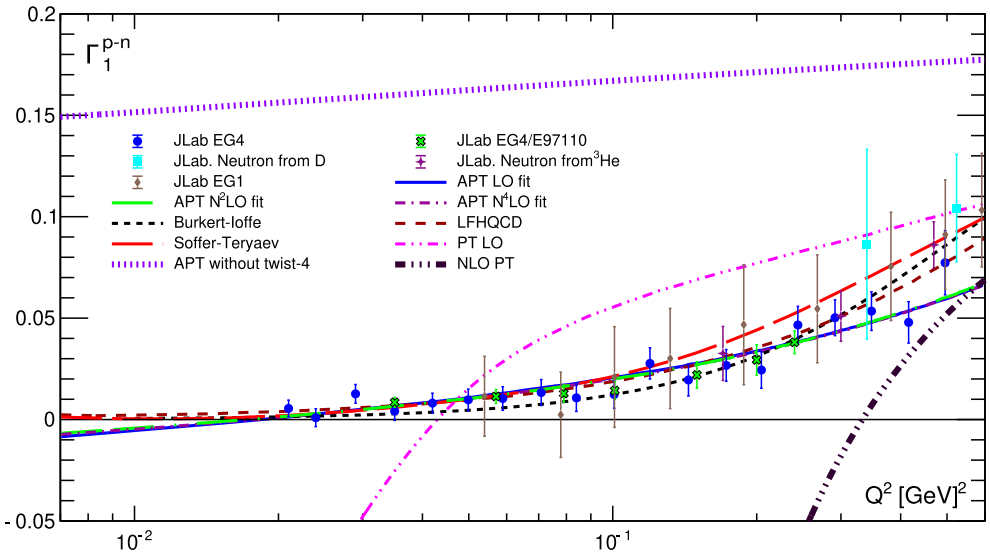

Figure 18. The results for $\Gamma_1^{p-n}(Q^2)$ in the first four orders of APT from fits of experimental data with Q^2 <0.6 GeV^2

10.3. Photoproduction

To understand the problem $\Gamma^{p-n}_{\rm MA,1}(Q^2 \to 0) < 0$, demonstrated above, we consider the photoproduction case. In the k-th order of MA QCD

$$A^{(k)}_{\rm MA}(Q^2=0) \equiv \tilde{A}^{(k)}_{{\rm MA},m=1}(Q^2=0) = 1, \;\; \tilde{A}^{(k)}_{{\rm MA},m} = 0, \;\; \text{when} \;\; m > 1 \tag{113}$$

and, so, we have

$$D_{\rm MA,BS}(Q^2=0) = \frac{4}{\beta_0} \;\; \text{and, hence,} \;\; \Gamma^{p-n}_{\rm MA,1}(Q^2=0) = \frac{g_A}{6}\left(1-\frac{4}{\beta_0}\right) + \hat{\mu}_{\rm MA,4}\,. \tag{114}$$

The finitness of cross-section in the real photon limit leads to [58]

$$\Gamma^{p-n}_{\rm MA,1}(Q^2=0) = 0 \;\; \text{and, thus,} \;\; \hat{\mu}^{php}_{\rm MA,4} = -\frac{g_A}{6}\left(1-\frac{4}{\beta_0}\right). \tag{115}$$

For $f = 3$, we have

$$\hat{\mu}^{php}_{\rm MA,4} = -0.118 \;\; \text{and, hence,} \;\; |\hat{\mu}^{php}_{\rm MA,4}| < |\hat{\mu}_{\rm MA,4}|, \tag{116}$$

shown in (106) and in Table 1.

So, as can be seen from Table 1, the finiteness of the cross section in the real photon limit is violated in our approaches. [11] This violation leads to negative values of $\Gamma^{p-n}_{\rm MA,1}(Q^2 \to 0)$. Note that this violation is less for experimental data sets with $Q^2 \le 0.6$GeV^2, where the obtained values for $|\hat{\mu}_{\rm MA,4}|$

[11] Note that the results for $\hat{\mu}_{\rm MA,4}$ were obtained taking into account only statistical uncertainties. When adding systematic uncertainties, the results for $\hat{\mu}^{php}_{\rm MA,4}$ and $\hat{\mu}_{\rm MA,4}$ are completely consistent with each other, but the predictive power of such an analysis is small.

 doi:10.20944/preprints202412.1263.v1

are essentially less then those obtained in the case of experimental data with $Q^2 \leq 5\text{GeV}^2$. Smaller values of $|\hat{\mu}_{\text{MA},4}|$ lead to negative values of $\Gamma^{p-n}_{\text{MA},1}(Q^2 \to 0)$, when $Q^2 \leq 0.02\text{GeV}^2$ (see Figure 4).

10.4. Gerasimov-Drell-Hearn and Burkhardt-Cottingham Sum Rules

Now we plan to improve this analysis by involving the result (110) at low Q^2 values and also taking into account the "massive" twist-six term, similar to the twist-four shown in Eq. (105).

Moreover, we take into account also the GDH and BC sum rules, which lead to (see [58,59,78,79])

$$\frac{d}{dQ^2}\Gamma^{p-n}_{\text{MA},1}(Q^2=0) = G, \;\; G = \frac{\mu_n^2 - (\mu_p - 1)^2}{8M_p^2} = 0.0631\,, \tag{117}$$

where $\mu_n = -1.91$ and $\mu_p = 2.79$ are proton and neutron magnetic moments, respectively, and $M_p = 0.938$ GeV is a nucleon mass. Note that the value of G is small.

In agreement with the definition (12), we have that

$$Q^2 \frac{d}{dQ^2}\tilde{A}_n(Q^2) \sim \tilde{A}_{n+1}(Q^2)\,. \tag{118}$$

Then, for $Q^2 \to 0$ we obtain at any n value, that

$$Q^2 \frac{d}{dQ^2}\tilde{A}_n(Q^2) \to 0\,, \tag{119}$$

but very slowly, that the derivative

$$\frac{d}{dQ^2}\tilde{A}_n(Q^2 \to 0) \to \infty\,. \tag{120}$$

Thus, after application the derivative d/dQ^2 for $\Gamma^{p-n}_{\text{MA},1}(Q^2)$, every term in $D_{\text{MA,BS}}(Q^2)$ becomes to be divergent at $Q^2 \to 0$. To produce finitness at $Q^2 \to 0$ for the l.h.s. of (117), we can assume the relation between twist-two and twist-four terms, that leads to the appearance of a new contribution

$$-\frac{g_A}{6}\, D_{\text{MA,BS}}(Q^2) + \frac{\hat{\mu}_{\text{MA},4} M^2}{Q^2 + M^2}\, D_{\text{MA,BS}}(Q^2)\,, \tag{121}$$

which can be done to be regular at $Q^2 \to 0$.

The form (121) suggests the following idea about a modification of $\Gamma^{p-n}_{\text{MA},1}(Q^2)$ in (110):

$$\Gamma^{p-n}_{\text{MA},1}(Q^2) = \frac{g_A}{6}\left(1 - D_{\text{MA,BS}}(Q^2) \cdot \frac{Q^2}{Q^2 + M^2}\right) + \frac{\hat{\mu}_{\text{MA},4} M^2}{Q^2 + M^2} + \frac{\hat{\mu}_{\text{MA},6} M^4}{(Q^2 + M^2)^2}, \tag{122}$$

where we added the "massive" twist-six term and introduced different masses in both higher-twist terms and into the modification factor $Q^2/(Q^2 + M^2)$.

The finitness of cross-section in the real photon limit leads now to [58]

$$\Gamma^{p-n}_{\text{MA},1}(Q^2=0) = 0 = \frac{g_A}{6} + \hat{\mu}_{\text{MA},4} + \hat{\mu}_{\text{MA},6} \tag{123}$$

and, thus, we have

$$\hat{\mu}_{\text{MA},4} + \hat{\mu}_{\text{MA},6} = -\frac{g_A}{6} \approx -0.21205 \tag{124}$$

From Eq. (122) and condition (117), we obtain

$$-\frac{g_A}{6} \cdot D_{\text{MA,BS}}(Q^2=0) - \hat{\mu}_{\text{MA},4} - 2\hat{\mu}_{\text{MA},6} = GM^2\,, \tag{125}$$

 doi:10.20944/preprints202412.1263.v1

where $D_{\rm MA,BS}(Q^2=0)=4/\beta_0$ (see Eq. (114)).

Using $f=3$ (i.e. $\beta_0=9$), we have

$$\hat{\mu}_{\rm MA,4}+2\hat{\mu}_{\rm MA,6}=-G\,M^2-\frac{2g_A}{3\beta_0}=-G\,M^2-\frac{2g_A}{27}\approx -G\,M^2-0.0945 \tag{126}$$

Taking the results (123) and (126) together, we have at the end the following results:

$$\begin{aligned}\hat{\mu}_{\rm MA,6}&=-G\,M^2+\frac{5g_A}{54}=-G\,M^2+0.1182,\\ \hat{\mu}_{\rm MA,4}&=-\frac{g_A}{6}-\hat{\mu}_{\rm MA,6}=G\,M^2-\frac{7g_{A/V}}{27}=G\,M^2-0.3309\,.\end{aligned} \tag{127}$$

Since the value of G is small, so $\hat{\mu}_{\rm MA,4}<0$ and $\hat{\mu}_{\rm MA,6}\approx -0.36\hat{\mu}_{\rm MA,4}>0$.

The fitting results of theoretical predictions based on Eq. (122) with $\hat{\mu}_{\rm MA,4}$ and $\hat{\mu}_{\rm MA,6}$ done in (127), are presented in Table 2 and on Figures 19 and 20.

As one can see in Table 2, the obtained results for M^2 are different if we take the full data set and the limited one with Q^2 <0.6 GeV^2. However, the difference is significantly less than it was in Table 1. Moreover, the results obtained in the fits using the full data set and shown in Tables 1 and 2 are quite similar, too.

We also see some similarities between the results shown in Figures 16 and 19. The difference appears only at small Q^2 values, as can be seen in Figures 17 and 20.

Table 2. The values of the fit parameters.

	M^2 [GeV^2] for $Q^2\leq$ 5 GeV^2 (for $Q^2\leq$ 0.6 GeV^2)	χ^2/(d.o.f.) for $Q^2\leq$ 5 GeV^2 (for $Q^2\leq$ 0.6 GeV^2)
LO	0.383 ± 0.014 (0.576 ± 0.046)	0.572 (0.575)
NLO	0.394 ± 0.013 (0.464 ± 0.039)	0.586 (0.590)
N^{2}LO	0.328 ± 0.014 (0.459 ± 0.038)	0.617 (0.584)
N^{3}LO	0.330 ± 0.014 (0.464 ± 0.039)	0.629 (0.582)
N^{4}LO	0.331 ± 0.013 (0.465 ± 0.039)	0.625 (0.584)

Figure 20 also shows that the results of fitting the full set of experimental data are in better agreement with the data at $Q^2\geq 0.55$GeV^2, as it should be, since these data are involved in the analyses of the full set of experimental data.

Preprints.org (www.preprints.org) | NOT PEER-REVIEWED | Posted: 16 December 2024 doi:10.20944/preprints202412.1263.v1

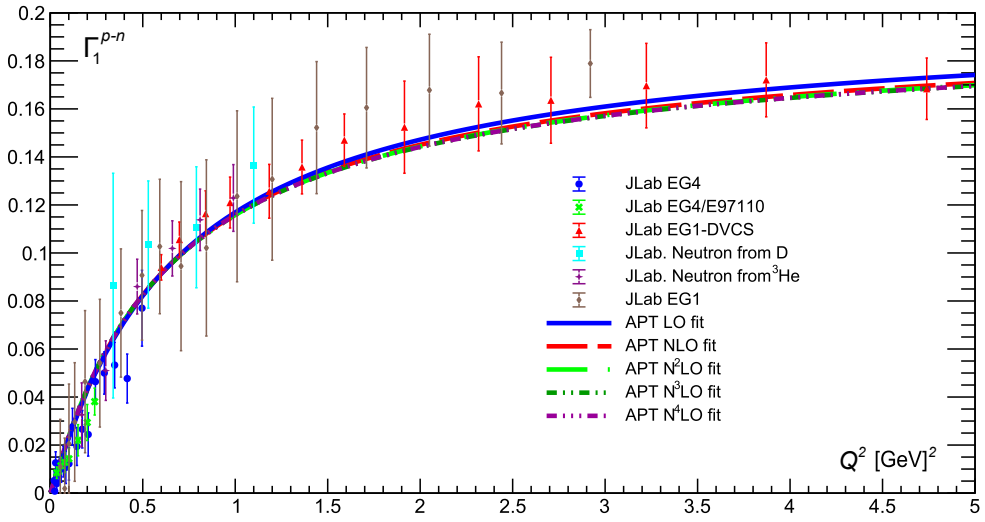

Figure 19. The results for $\Gamma_1^{p-n}(Q^2)$ (122) in the first four orders of APT.

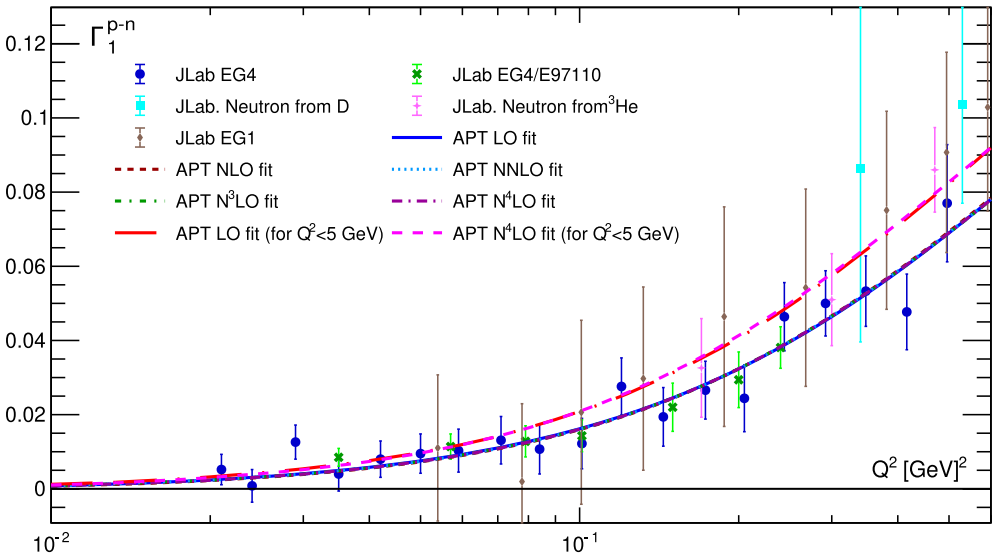

Figure 20. As in Figure 19 but for Q^2 <0.6 GeV^2

The results shown in Tables 1 and 2 are not changes practically when heavy quark contributions [80] were added in consideration (see [81]).

11. Conclusions

In this paper we presented an overview of fractional analytic QCD and its application for Higgs-boson decay into a bottom-antibottom pair and for the polarized Bjorken sum rule.

We have considered $1/L$-expansions of ν-derivatives of the strong couplant a_s expressed as combinations of operators $\hat{R}_m$ (14) applied to the LO couplant $a_s^{(1)}$. Applying the same operators to the ν-derivatives of the LO MA couplant $A_{\rm MA}^{(1)}$, we obtained four different representations for the ν-derivatives of the MA couplants, i.e. $\tilde{A}_{{\rm MA},\circ}^{(i)}$, in each i-order of perturbation theory: one form contains a combination of Polylogariths; the other contains an expansion of the generalized Euler ζ-function,

 doi:10.20944/preprints202412.1263.v1

and the third is based on dispersion integrals containing the LO spectral function. We also obtained a fourth representation based on the dispersion integral containing the i-order spectral function. All results are presented up to the 5th order of perturbation theory, where the corresponding coefficients of the QCD β-function are well known (see [2,3]).

The high-order corrections are negligible in the $Q^2 \to 0$ and $Q^2 \to \infty$ asymptotics and are nonzero in the vicinity of the point $Q^2 = \Lambda^2$. Thus, in fact, they are really only small corrections to the LO MA couplant $A^{(1)}_{\mathrm{MA},\circ}(Q^2)$. This proves the possibility of expansions of high-order couplants $A^{(i)}_{\mathrm{MA},\circ}(Q^2)$ via the LO couplants $A^{(1)}_{\mathrm{MA},\circ}(Q^2)$, which was done in Ref. [9], as well as the possibility of various approximations used in [28,38–40].

As can be clearly seen, all our results (*up to the 5th order of perturbation theory*) have a compact form and do not contain complicated special functions, such as the Lambert W-function [82], which already appears at the two-loop order as an exact solution to the usual couplant and which was used to evaluate MA couplants in [83].

Applying the same operators to the ν-derivatives of the LO MA couplant $U^{(1)}_{\mathrm{MA}}$, we obtained two different representations (see Eqs. (29) and (71)) for the ν-derivatives of the MA couplants, i.e. $\tilde{U}^{(i)}_{\mathrm{MA},\circ}$ introduced for timelike processes, in each i-order of perturbation theory: one form contains a combinations of trigonometric functions, and the other is based on dispersion integrals containing the i-order spectral function. All results are presented up to the 5th order of perturbation theory, where the corresponding coefficients of the QCD β-function are well known (see [2,3]).

As in the case of $\tilde{A}^{(i)}_{\mathrm{MA},\circ}$ [18] applied in the Euclidean space, high-order corrections for $\tilde{U}^{(i)}_{\mathrm{MA},\circ}$ are negligible in the $s \to 0$ and $s \to \infty$ limits and are nonzero in the vicinity of the point $s = \Lambda^2$. Thus, in fact, there are actually only small corrections to the LO MA couplant $U^{(1)}_{\mathrm{MA},\circ}(s)$. In particular, this proves the possibility of expansions of high-order couplants $U^{(i)}_{\mathrm{MA},\circ}(s)$ via the LO couplants $U^{(1)}_{\mathrm{MA},\circ}(s)$, which was done in Ref. [9].

As an example, we examined the Higgs boson decay into a $b\bar{b}$ pair and obtained results are in good agreement with the Standard Model expectations [49] and with the experimental data [50,51]. Moreover, our results also in good agreement with studies based on the Principle Maximum Conformality [47].

As a second application, we considered the Bjorken sum rule $\Gamma^{p-n}_1(Q^2)$ in the framework of MA and perturbative QCD and obtained results similar to those obtained in previous studies [21, 38,39,60,61] for the first 4 orders of PT. The results based on the conventional PT do not agree with the experimental data. For some Q^2 values, the PT results become negative, since the high-order corrections are large and enter the twist-two term with a minus sign. APT in the minimal version leads to a good agreement with experimental data when we used the "massive" version (110) for the twist-four contributions.

Examining low Q^2 behaviour, we found that there is a disagreement between the results obtained in the fits and application of MA QCD to photoproduction. The results of fits extented to low Q^2 lead to the negative values for Bjorken sum rule $\Gamma^{p-n}_{\mathrm{MA},1}(Q^2)$: $\Gamma^{p-n}_{\mathrm{MA},1}(Q^2 \to 0) < 0$ that contrary to the finitness of cross-section in the real photon limit, which leads to $\Gamma^{p-n}_{\mathrm{MA},1}(Q^2 \to 0) = 0$. Note that fits of experimental data at low Q^2 values (we used $Q^2 < 0.6\ \mathrm{GeV}^2$) lead to less magnitudes of negative values for $\hat{\mu}_{\mathrm{MA},4}$ (see Tables 1 and 2).

To solve the problem we considered low Q^2 modifications of OPE formula for $\Gamma^{p-n}_{\mathrm{MA},1}(Q^2)$. Considering carefully one of them, Eq. (122), we find good agreement with full sets of experimental data for Bjorken sum rule $\Gamma^{p-n}_{\mathrm{MA},1}(Q^2)$ and also with its $Q^2 \to 0$ limit, i.e. with photoproduction. We see also good agreement with phenomenological modeles [77–79], especially with LFHQCD [76].

Acknowledgments: We are grateful to Gorazd Cvetic for initiating these studies and collaborating at the initial stage and Alexander Nesterenko for the information about the 5-loop spectral function $r^{(4)}_{\mathrm{pt}}(s)$ calculated in his paper [37]. We are alsograteful to Alexandre P. Deur for information about new experimental data in Ref. [68] and Johannes Blumlein for initiating the consideration of the contribution of heavy quarks. Authors thank Konstantin Chetyrkin, Andrei Kataev and Sergey Mikhailov for careful discussions. This work was supported in part by

 doi:10.20944/preprints202412.1263.v1

the Foundation for the Advancement of Theoretical Physics and Mathematics "BASIS". One of us (I.A.Z.) is supported by the Directorate of Postgraduate Studies of the Technical University of Federico Santa Maria.

Appendix A. Details of Evaluation of the Fractional Derivatives

Taking the results (7) of the couplant $a_s(Q^2)$ we have the following results for the $1/L$-expansion of its ν-powers:

$$\left(a_{s,0}^{(1)}(Q^2)\right)^\nu = \frac{1}{L_0^\nu}, \;\; \left(a_{s,i}^{(i+1)}(Q^2)\right)^\nu = \left(a_{s,i}^{(1)}(Q^2)\right)^\nu + \sum_{m=2}^{i} \delta_{\nu,i}^{(m)}(Q^2), \;\; (i = 0, 1, 2, ...) \tag{A1}$$

where L_k is defined in Eq. (8) and

$$\delta_{nu,k}^{(2)}(Q^2) = -\frac{b_1 \nu \ln L_k}{L_k^{\nu+1}}, \;\; \delta_{\nu,k}^{(3)}(Q^2) = \frac{1}{L_k^{\nu+2}} \left[b_1^2 \left(\frac{\nu+1}{2} \ln^2 L_k - \ln L_k - 1\right) + b_2\right], \tag{A2}$$

which is consistent with the expansions made in Refs. [7,8].

The $(\nu-1)$-derivative $\tilde{a}_\nu(Q^2)$ is related with the $\nu + l$ $(l = 0, 1, 2, ...)$ powers as follows

$$\tilde{a}_\nu(Q^2) = a_s^\nu(Q^2) + k_1(\nu) a_s^{\nu+1}(Q^2) + k_2(\nu) a_s^{\nu+2}(Q^2) + O(a_s^{\nu+3}), \tag{A3}$$

where (see [34])

$$k_1(\nu) = \nu b_1 \, B_1(\nu), \;\; k_2(\nu) = \nu(\nu+1) \left(b_2 \, B_2(\nu) + \frac{b_1^2}{2} \, B_{1,1}(\nu)\right), \tag{A4}$$

with

$$B_1(\nu) = S_1(\nu) - 1, \;\; B_2(\nu) = \frac{\nu - 1}{2(\nu+1)}, \;\; B_{1,1}(\nu) = Z_2(\nu+1) - 2S_1(\nu) + 1, \;\; , \tag{A5}$$

and

$$Z_1(\nu) \equiv S_1(\nu) = \Psi(1+\nu) + \gamma_E, \;\; S_2(\nu) = \zeta_2 - \Psi'(1+\nu), \;\; Z_2(\nu) = S_1^2(\nu) - S_2(\nu), \tag{A6}$$

with Euler constant γ_E and Euler function ζ_2. The expression for $Z_k(\nu)$ with arbitrary k can be found in [34].

After some calculations, we have

$$\tilde{a}_{\nu,0}^{(1)}(Q^2) = \frac{1}{L_0^\nu}, \;\; \tilde{a}_{\nu,i}^{(i+1)}(Q^2) = \tilde{a}_{\nu,i}^{(1)}(Q^2) + \sum_{m=1}^{i} C_m^{\nu+m} \, \tilde{\delta}_{\nu,i}^{(m+1)}(Q^2), \tag{A7}$$

where

$$\tilde{\delta}_{\nu,k}^{(m+1)}(Q^2) = R_{m,k} \, \frac{1}{L_k^{\nu+m}} \tag{A8}$$

and

$$R_{1,k} = b_1 \left[\hat{Z}_1(\nu) - \ln L_k\right], \;\; R_{2,k} = b_2 + b_1^2 \left[\ln^2 L_k - 2\hat{Z}_1(\nu+1) \ln L_k + \hat{Z}_2(\nu+1)\right] \tag{A9}$$

and $C_m^{\nu+m}$ is given in Eq. (13) and

$$\hat{Z}_k(\nu) = \sum_{m=0}^{k} \frac{(-1)^m \, k!}{m!(k-m)!} \, Z_{k-m}(\nu), \;\; Z_0(\nu) = 1, \tag{A10}$$

with

$$\hat{Z}_1(\nu) = Z_1(\nu) - 1, \;\; \hat{Z}_2(\nu) = Z_2(\nu) - 2Z_1(\nu) + 1, \tag{A11}$$

 doi:10.20944/preprints202412.1263.v1

where $Z_i(\nu)$ are defined in Eq. (A6).

It is convenient to introduce the operators $\hat{R}_i$ (13), which can be obtained as $\hat{R}_i = R_{i,k}\big(\ln L_k \to -d/(d\nu)\big)$. In this case, we proceed to the results (13) and (14) of the main text.

It is convenient to express also a_s^ν through $\tilde{a}_{\nu+m}$. Considering Ref. [34] we have

$$a_s^\nu = \tilde{a}_\nu + \sum_{m\geq 1} \tilde{k}_m(\nu)\, \tilde{a}_{\nu+m}\,, \tag{A12}$$

where

$$\begin{aligned}
&\tilde{k}_1(\nu) = -\nu b_1 \tilde{B}_1(\nu),\\
&\tilde{k}_2(\nu) = \nu(\nu+1)\left(-b_2\tilde{B}_2(\nu) + \frac{b_1^2}{2}\tilde{B}_{1,1}(\nu)\right),,
\end{aligned} \tag{A13}$$

where

$$\tilde{B}_1(\nu) = \tilde{Z}_1(\nu) - 1,\;\; \tilde{B}_2(\nu) = \frac{\nu-1}{2(\nu+1)},\;\; \tilde{B}_{1,1}(\nu) = \tilde{Z}_2(\nu) - 2\tilde{Z}_1(\nu+1) + 1, \tag{A14}$$

and

$$\tilde{Z}_1(\nu) = S_1(\nu),\;\; \tilde{Z}_2(\nu) = S_1^2(\nu) + S_2(\nu),$$

For arbitrary ν values, $S_i(\nu)$ are expressed through Polygamma-functions (see (A6)). In the case of integer $\nu = n$,

$$S_i(n) = \sum_{m=1}^{n} \frac{1}{m^i}\,. \tag{A15}$$

Appendix B. Alternative Form for the Couplants $\tilde{A}^{(i+1)}_{\mathbf{MA},\overset{\circ}{,}i}(Q^2)$

Using the series representation (52), the functions $\zeta(n, -\nu - r - k)$ in (51) are not so good defined at large r values and by $\zeta(n, \nu + r + k)$ and we will replace them the using the result (43) as

$$\zeta(\nu - r) = -\frac{\Gamma(\nu+r+1)}{\pi(2\pi)^{\nu+r}}\,\tilde{\zeta}(\nu+r+1),\;\; \tilde{\zeta}(\nu+r+1) = \sin\Big[\frac{\pi}{2}(\nu+r)\Big]\,\zeta(\nu+r+1)\,. \tag{B1}$$

After come calculations we have

$$\tilde{\delta}^{(m+1)}_{\mathrm{MA},\nu,k}(Q^2) = \frac{1}{\Gamma(\nu+m)}\sum_{r=0}^{\infty}\frac{\Gamma(\nu+r+m)}{\pi(2\pi)^{\nu+r+m-1}}\,Q_m(\nu+r+m)\,\frac{(-L_k)^r}{r!} \tag{B2}$$

where

$$\begin{aligned}
Q_1(\nu+r+1) &= b_1\Big[\tilde{Z}_1(\nu+r)\tilde{\zeta}(\nu+r+1) + \tilde{\zeta}_1(\nu+r+1)\Big],\\
Q_2(\nu+r+2) &= b_2\tilde{\zeta}(\nu+r+2) + b_1^2\Big[\tilde{\zeta}_2(\nu+r+2) + 2\tilde{Z}_1(\nu+r+1)\tilde{\zeta}_1(\nu+r+2)\\
&\quad + \tilde{Z}_1(\nu+r+1)\tilde{\zeta}(\nu+r+2)\Big],
\end{aligned} \tag{B3}$$

with (see also (A6)

$$\begin{aligned}
&\overline{Z}_2(\nu) = \overline{S}_1^2(\nu) - S_2(\nu),\\
&\overline{Z}_1(\nu) \equiv \overline{S}_1(\nu) = \Psi(1+\nu) + \gamma_{\mathrm{E}} - \ln(2\pi),\;\; S_2(\nu) = \zeta_2 - \Psi'(1+\nu),
\end{aligned} \tag{B4}$$

 doi:10.20944/preprints202412.1263.v1

and (see also (A11))

$$\tilde{Z}_1(\nu) = \overline{Z}_1(\nu) - 1,\ \ \tilde{Z}_2(\nu) = \overline{Z}_2(\nu) - 2\overline{Z}_1(\nu) + 1,\ \ \tilde{Z}_3(\nu) = \overline{Z}_3(\nu) - 3\overline{Z}_2(\nu) + 3\overline{Z}_1(\nu) - 1,$$
$$\tilde{Z}_4(\nu) = \overline{Z}_4(\nu) - 4\overline{Z}_3(\nu) + 6\overline{Z}_2(\nu) - 4\overline{Z}_1(\nu) + 1\,. \tag{B5}$$

Moreover we use here

$$\tilde{\zeta}_k(\nu) = \frac{d^k}{(d\nu)^k}\,\tilde{\zeta}(\nu)\,. \tag{B6}$$

Using the definition of $\tilde{\zeta}_k(\nu)$ in (B1), we have

$$\tilde{\zeta}_1(\nu+r+1) = \sin\Big[\frac{\pi}{2}(\nu+r)\Big]\,\zeta_1(\nu+r+1) + \frac{\pi}{2}\,\cos\Big[\frac{\pi}{2}(\nu+r)\Big]\,\zeta(\nu+r+1)\,,$$
$$\tilde{\zeta}_2(\nu+r+1) = \sin\Big[\frac{\pi}{2}(\nu+r)\Big]\,\Big(\zeta_2(\nu+r+1) - \frac{\pi^2}{4}\,\zeta(\nu+r+1)\Big)$$
$$+\frac{\pi}{2}\,\cos\Big[\frac{\pi}{2}(\nu+r)\Big]\,\zeta_1(\nu+r+1)\,, \tag{B7}$$

where $\zeta_k(\nu)$ are given in Eq. (52) of the main text.

So, we can rewrite the results (B2) with

$$Q_m(\nu+r+m) = \sin\Big[\frac{\pi}{2}(\nu+r+m-1)\Big]\,Q_{ma}(\nu+r+m)$$
$$+\frac{\pi}{2}\,\cos\Big[\frac{\pi}{2}(\nu+r+m-1)\Big]\,Q_{mb}(\nu+r+m)\,, \tag{B8}$$

where

$$Q_{1a}(\nu+r+1) = b_1\Big[\tilde{Z}_1(\nu+r)\zeta(\nu+r+1) + \zeta_1(1,\nu+r+1)\Big],$$
$$Q_{1b}(\nu+r+1) = b_1\zeta(\nu+r+1),$$
$$Q_{2a}(\nu+r+2) = b_2\zeta(\nu+r+2) + b_1^2\Big[\zeta_2(\nu+r+2) + 2\tilde{Z}_1(\nu+r+1)\zeta_1(\nu+r+2)$$
$$+\Big(\tilde{Z}_1(\nu+r+1) - \frac{\pi^2}{4}\Big)\zeta(\nu+r+2)\Big],$$
$$Q_{2b}(\nu+r+2) = 2b_1^2\Big[\tilde{Z}_1(\nu+r+1)\zeta(\nu+r+2) + \zeta_1(\nu+r+2)\Big]\,. \tag{B9}$$

Appendix C. $\overline{m}_b^2(Q^2)$

Here we present evaluation of $\overline{m}_b^2(Q^2)$, which has the form

$$\overline{m}_b^2(Q^2) = \overline{m}_b^2(Q^2)\,\exp\left[2\int_{\bar{a}_s(Q_0^2)}^{\bar{a}_s(Q^2)}\frac{\gamma_m(a)}{\beta_(a)}\right],\ \ \bar{a}_s(Q^2) = \frac{\alpha_s(Q^2)}{4\pi}\,, \tag{C1}$$

where

$$\gamma_m(a) = -\sum_{k=0}\gamma_k a^{k+1} = -\gamma_0 a\big(1 + \sum_{k=1}\delta_k a^k\big),\ \ \delta_k = \frac{\gamma_k}{\gamma_0}\,,$$
$$\beta(a) = -\sum_{k=0}\beta_k a^{k+2} = -\beta_0 a^2\big(1 + \sum_{k=1}c_k a^k\big),\ \ c_k = \frac{\beta_k}{\beta_0}\,. \tag{C2}$$

Evaluating the integral in (C1) we have the following results (see, e.g., also Refs. [8,84])

$$\overline{m}_b^2(Q^2) = \overline{m}_b^2(Q^2)\,\frac{\bar{a}_s^d(Q^2)}{\bar{a}_s^d(Q_0^2)}\,\frac{T(\bar{a}_s(Q^2))}{T(\bar{a}_s(Q_0^2))}\,, \tag{C3}$$

 doi:10.20944/preprints202412.1263.v1

where

$$d = \frac{2\gamma_0}{\beta_0}, \;\; T(\bar{a}_s) = \exp[\sum_{k=1}^{k=4} \frac{e_k}{k} \bar{a}_s^k] \tag{C4}$$

and

$$\begin{aligned} &e_1 = d\Delta_1, \;\; e_2 = d(\Delta_2 - c_1\Delta_1), \;\; e_3 = d(\Delta_3 - c_1\Delta_2 - \tilde{c}_2\Delta_1), \\ &e_4 = d(\Delta_4 - c_1\Delta_3 - \tilde{c}_2\Delta_2 - \tilde{c}_3\Delta_1)\,, \end{aligned} \tag{C5}$$

with

$$\Delta_i = \delta_i - c_i, \;\; \tilde{c}_2 = c_2 - c_1^2, \;\; \tilde{c}_3 = c_3 - 2c_1c_2 + c_1^3 \tag{C6}$$

The result for $T(\bar{a}_s)$ can be rewritten as

$$T(\bar{a}_s) = 1 + \sum_{k=1}^{k=4} \frac{\tilde{e}_k}{k} \bar{a}_s^k\,, \tag{C7}$$

where

$$\begin{aligned} &\tilde{e}_1 = e_1, \;\; \tilde{e}_2 = e_2 + e_1^2, \;\; \tilde{e}_3 = e_3 + \frac{3}{2}e_1e_2 + \frac{1}{2}e_1^3, \\ &\tilde{e}_3 = e_4 + e_2^2 + \frac{4}{3}e_1e_3 + \frac{1}{2}e_1^3 + e_1^2e_2 + \frac{1}{6}e_1^4, \end{aligned} \tag{C8}$$

References

1. N. N. Bogolyubov and D. V. Shirkov, Intersci. Monogr. Phys. Astron. **3** (1959), 1-720
2. P. A. Baikov, K. G. Chetyrkin and J. H. Kühn, Phys. Rev. Lett. **118** (2017) no.8, 082002
3. F. Herzog, B. Ruijl, T. Ueda, J. A. M. Vermaseren and A. Vogt, JHEP **02** (2017), 090
4. T. Luthe, A. Maier, P. Marquard and Y. Schroder, JHEP **10** (2017), 166 K. G. Chetyrkin, G. Falcioni, F. Herzog and J. A. M. Vermaseren, JHEP **10** (2017), 179
5. D. V. Shirkov and I. L. Solovtsov, Phys. Rev. Lett. **79** (1997), 1209-1212; D. V. Shirkov, Theor. Math. Phys. **127** (2001), 409-423 Eur. Phys. J. C **22** (2001), 331-340
6. K. A. Milton, I. L. Solovtsov and O. P. Solovtsova, Phys. Lett. B **415** (1997), 104-110
7. A. P. Bakulev, S. V. Mikhailov and N. G. Stefanis, Phys. Rev. D **72** (2005), 074014 [Erratum-ibid. D **72** (2005), 119908]
8. A. P. Bakulev, S. V. Mikhailov and N. G. Stefanis, Phys. Rev. D **75** (2007), 056005 [erratum: Phys. Rev. D **77** (2008), 079901]
9. A. P. Bakulev, S. V. Mikhailov and N. G. Stefanis, JHEP **06** (2010), 085
10. M. R. Pennington and G. G. Ross, Phys. Lett. B **102**, 167-171 (1981); M. R. Pennington, R. G. Roberts and G. G. Ross, Nucl. Phys. B **242**, 69-80 (1984); R. Marshall, Z. Phys. C **43**, 595 (1989).
11. N. V. Krasnikov and A. A. Pivovarov, Phys. Lett. B **116**, 168-170 (1982); A. V. Radyushkin, JINR Rapid Commun. **78**, 96-99 (1996) [arXiv:hep-ph/9907228 [hep-ph]].
12. M. B. Gay Ducati, F. Halzen and A. A. Natale, Phys. Rev. D **48** (1993), 2324-2328; A. C. Mattingly and P. M. Stevenson, Phys. Rev. Lett. **69** (1992), 1320-1323 Phys. Rev. D **49** (1994), 437-450
13. A. V. Kotikov, A. V. Lipatov and N. P. Zotov, J. Exp. Theor. Phys. **101**, 811-816 (2005)
14. N. N. Bogolyubov, A. A. Logunov and D. V. Shirkov, Sov.Phys.JETP 10 (1960) 3, 574-581; P. J. Redmond, Phys. Rev. **112** (1958), 1404.
15. G. Cvetic and C. Valenzuela, Braz. J. Phys. **38** (2008), 371-380
16. A. P. Bakulev, Phys. Part. Nucl. **40** (2009), 715-756; N. G. Stefanis, Phys. Part. Nucl. **44** (2013), 494-509
17. A. V. Nesterenko, Int. J. Mod. Phys. A **18** (2003), 5475-5520; A. V. Nesterenko and J. Papavassiliou, Phys. Rev. D **71** (2005), 016009
18. A. V. Kotikov and I. A. Zemlyakov, J. Phys. G **50** (2023) no.1, 015001
19. A. V. Kotikov and I. A. Zemlyakov, Phys. Rev. D **107**, no.9, 094034 (2023)
20. A. V. Kotikov and I. A. Zemlyakov, [arXiv:2207.01330 [hep-ph]]; Phys. Part. Nucl. **55**, no.4, 863-867 (2024)

21. I. R. Gabdrakhmanov, N. A. Gramotkov, A. V. Kotikov, D. A. Volkova and I. A. Zemlyakov, JETP Lett. 118 (2023) 7, 478-482 [Pisma Zh. Eksp. Teor. Fiz. **118**, no.7, 491-492 (2023)]
22. I. R. Gabdrakhmanov, N. A. Gramotkov, A. V. Kotikov, O. V. Teryaev, D. A. Volkova and I. A. Zemlyakov, [arXiv:2404.01873 [hep-ph]].
23. B. G. Shaikhatdenov, A. V. Kotikov, V. G. Krivokhizhin and G. Parente, Phys. Rev. D **81**, 034008 (2010) [erratum: Phys. Rev. D **81**, 079904 (2010)]; V. G. Krivokhizhin and A. V. Kotikov, Phys. Atom. Nucl. **68**, 1873-1903 (2005)
24. Particle Data Group collaboration, P.A. Zyla et al., Review of Particle Physics, PTEP **2020** (2020) 083C01.
25. K. G. Chetyrkin, J. H. Kuhn and C. Sturm, Nucl. Phys. B **744** (2006), 121-135; Y. Schroder and M. Steinhauser, JHEP **01** (2006), 051; B. A. Kniehl, A. V. Kotikov, A. I. Onishchenko and O. L. Veretin, Phys. Rev. Lett. **97** (2006), 042001
26. D. d'Enterria, *et al.* [arXiv:2203.08271 [hep-ph]].
27. H. M. Chen, L. M. Liu, J. T. Wang, M. Waqas and G. X. Peng, Int. J. Mod. Phys. E **31** (2022) no.02, 2250016
28. A. Y. Illarionov, A. V. Kotikov and G. Parente Bermudez, Phys. Part. Nucl. **39** (2008), 307-347
29. S. Chekanov et al., ZEUS Collab., Eur. Phys. J. C 21, 443 (2001).
30. G. Cvetic and C. Valenzuela, J. Phys. G **32** (2006), L27
31. G. Cvetic and C. Valenzuela, Phys. Rev. D **74** (2006), 114030 [erratum: Phys. Rev. D **84** (2011), 019902]
32. A. V. Kotikov and I. A. Zemlyakov, JETP Lett. **115** (2022) no.10, 565–56
33. G. Cvetic, R. Kogerler and C. Valenzuela, Phys. Rev. D **82** (2010), 114004
34. G. Cvetič and A. V. Kotikov, J. Phys. G **39** (2012), 065005
35. A. V. Kotikov and L. N. Lipatov, Nucl. Phys. B **582** (2000), 19-43; Nucl. Phys. B **661** (2003), 19-61; A. V. Kotikov, L. N. Lipatov, A. I. Onishchenko and V. N. Velizhanin, Phys. Lett. B **595** (2004), 521-529; L. Bianchi, V. Forini and A. V. Kotikov, Phys. Lett. B **725** (2013), 394-401
36. A. V. Nesterenko and C. Simolo, Comput. Phys. Commun. **181**, 1769-1775 (2010)
37. A. V. Nesterenko, Eur. Phys. J. C **77**, no.12, 844 (2017)
38. R. S. Pasechnik *et al.*, Phys. Rev. D **78** (2008), 071902; Phys. Rev. D **81** (2010), 016010; A. V. Kotikov and B. G. Shaikhatdenov, Phys. Part. Nucl. **45** (2014), 26-29
39. V. L. Khandramai *et al.*, Phys. Lett. B **706** (2012), 340-344
40. A. V. Kotikov, V. G. Krivokhizhin and B. G. Shaikhatdenov, Phys. Atom. Nucl. **75** (2012), 507-524; A. V. Sidorov and O. P. Solovtsova, Mod. Phys. Lett. A **29** (2014) no.36, 1450194
41. D. J. Broadhurst, A. L. Kataev and C. J. Maxwell, Nucl. Phys. B **592**, 247-293 (2001)
42. K. G. Chetyrkin, Phys. Lett. B **390**, 309-317 (1997)
43. P. A. Baikov, K. G. Chetyrkin and J. H. Kuhn, Phys. Rev. Lett. **96**, 012003 (2006); Acta Phys. Polon. B **48**, 2135 (2017)
44. K. G. Chetyrkin, B. A. Kniehl and A. Sirlin, Phys. Lett. B **402**, 359-366 (1997)
45. A. L. Kataev and V. T. Kim, Mod. Phys. Lett. A **9**, 1309-1326 (1994); PoS **ACAT08**, 004 (2008)
46. S. Q. Wang, X. G. Wu, X. C. Zheng, J. M. Shen and Q. L. Zhang, Eur. Phys. J. C **74** (2014) no.4, 2825
47. S. J. Brodsky and X. G. Wu, Phys. Rev. D **85** (2012), 034038 [erratum: Phys. Rev. D **86** (2012), 079903]; Phys. Rev. Lett. **109** (2012), 042002; S. J. Brodsky and L. Di Giustino, Phys. Rev. D **86** (2012), 085026; M. Mojaza, S. J. Brodsky and X. G. Wu, Phys. Rev. Lett. **110** (2013), 192001; S. J. Brodsky, M. Mojaza and X. G. Wu, Phys. Rev. D **89** (2014), 014027
48. J. M. Shen, Z. J. Zhou, S. Q. Wang, J. Yan, Z. F. Wu, X. G. Wu and S. J. Brodsky, [arXiv:2209.03546 [hep-ph]]; J. Yan, Z. F. Wu, J. M. Shen and X. G. Wu, [arXiv:2209.13364 [hep-ph]].
49. D. de Florian *et al.* [LHC Higgs Cross Section Working Group], [arXiv:1610.07922 [hep-ph]].
50. M. Aaboud *et al.* [ATLAS], Phys. Lett. B **786** (2018), 59-86
51. A. M. Sirunyan *et al.* [CMS], Phys. Rev. Lett. **121** (2018) no.12, 121801
52. I. I. Tsukerman, Phys. Atom. Nucl. **83** (2020) no.2, 219-227
53. J. D. Bjorken, Phys. Rev. **148**, 1467-1478 (1966); Phys. Rev. D **1**, 1376-1379 (1970)
54. A. Deur, S. J. Brodsky and G. F. De Téramond, [arXiv:1807.05250 [hep-ph]]
55. S. E. Kuhn, J. P. Chen and E. Leader, Prog. Part. Nucl. Phys. **63**, 1-50 (2009)
56. E. V. Shuryak and A. I. Vainshtein, Nucl. Phys. B **201**, 141 (1982)
57. I. I. Balitsky, V. M. Braun and A. V. Kolesnichenko, Phys. Lett. B **242**, 245-250 (1990) [erratum: Phys. Lett. B **318**, 648 (1993)]

58. O. Teryaev, Nucl. Phys. B Proc. Suppl. **245** (2013), 195-198; V. L. Khandramai, O. V. Teryaev and I. R. Gabdrakhmanov, J. Phys. Conf. Ser. **678** (2016) no.1, 012018
59. I. R. Gabdrakhmanov, O. V. Teryaev and V. L. Khandramai, J. Phys. Conf. Ser. **938** (2017) no.1, 012046
60. C. Ayala *et al.*, Int. J. Mod. Phys. A **33** (2018) no.18n19, 1850112; J. Phys. Conf. Ser. **938** (2017) no.1, 012055
61. C. Ayala *et al.*, Eur. Phys. J. C **78**, no.12, 1002 (2018); J. Phys. Conf. Ser. **1435** (2020) no.1, 012016
62. J. P. Chen, [arXiv:nucl-ex/0611024 [nucl-ex]]; J. P. Chen, A. Deur and Z. E. Meziani, Mod. Phys. Lett. A **20** (2005), 2745-2766
63. C. Ayala and A. Pineda, Phys. Rev. D **106**, no.5, 056023 (2022)
64. D. Kotlorz and S. V. Mikhailov, Phys. Rev. D **100**, no.5, 056007 (2019)
65. C. Ayala, C. Castro-Arriaza and G. Cvetič, Phys. Lett. B **848**, 138386 (2024); [arXiv:2312.13134 [hep-ph]].
66. P. A. Baikov, K. G. Chetyrkin and J. H. Kuhn, Phys. Rev. Lett. **101**, 012002 (2008)
67. Y. Aoki et al., arXiv:2111.09849 [hep-lat];
68. A. Deur *et al.* Phys. Lett. B **825**, 136878 (2022)
69. K. Abe *et al.* [E143 Collaboration], Phys. Rev. D **58**, 112003 (1998); K. Abe *et al.* [E154 Collaboration], Phys. Rev. Lett. **79**, 26-30 (1997); P. L. Anthony *et al.* [E142 Collaboration], Phys. Rev. D **54**, 6620-6650 (1996); P. L. Anthony *et al.* [E155 Collaboration], Phys. Lett. B **463**, 339-345 (1999); Phys. Lett. B **493**, 19-28 (2000).
70. B. Adeva *et al.* [Spin Muon Collaboration], Phys. Lett. B **302**, 533-539 (1993); Phys. Lett. B **412**, 414-424 (1997); D. Adams *et al.* [Spin Muon Collaboration (SMC)], Phys. Lett. B **329**, 399-406 (1994) [erratum: Phys. Lett. B **339**, 332-333 (1994)]; Phys. Lett. B **357**, 248-254 (1995) Phys. Lett. B **396**, 338-348 (1997); Phys. Rev. D **56**, 5330-5358 (1997)
71. E. S. Ageev *et al.* [COMPASS Collaboration], Phys. Lett. B **612**, 154-164 (2005); Phys. Lett. B **647**, 330-340 (2007); M. G. Alekseev *et al.* [COMPASS Collaboration], Phys. Lett. B **690**, 466-472 (2010); C. Adolph *et al.* [COMPASS Collaboration], Phys. Lett. B **753**, 18-28 (2016); Phys. Lett. B **769**, 34-41 (2017); Phys. Lett. B **781**, 464-472 (2018).
72. K. Ackerstaff *et al.* [HERMES Collaboration], Phys. Lett. B **404**, 383-389 (1997); A. Airapetian *et al.* [HERMES Collaboration], Phys. Lett. B **442**, 484-492 (1998); Phys. Rev. D **75**, 012007 (2007)
73. A. Deur *et al.* Phys. Rev. Lett. **93**, 212001 (2004); Phys. Rev. D **78**, 032001 (2008) Phys. Rev. D **90**, no.1, 012009 (2014)
74. K. Slifer *et al.* [Resonance Spin Structure], Phys. Rev. Lett. **105**, 101601 (2010)
75. A. L. Kataev, JETP Lett. **81**, 608-611 (2005); Mod. Phys. Lett. A **20**, 2007-2022 (2005)
76. S. J. Brodsky, G. F. de Teramond, H. G. Dosch and J. Erlich, Phys. Rept. **584**, 1-105 (2015)
77. V. D. Burkert and B. L. Ioffe, Phys. Lett. B **296**, 223-226 (1992); J. Exp. Theor. Phys. **78**, 619-622 (1994)
78. J. Soffer and O. Teryaev, Phys. Rev. Lett. **70**, 3373-3375 (1993); Phys. Rev. D **70**, 116004 (2004)
79. R. S. Pasechnik, J. Soffer and O. V. Teryaev, Phys. Rev. D **82**, 076007 (2010)
80. J. Blümlein, G. Falcioni and A. De Freitas, Nucl. Phys. B **910**, 568-617 (2016)
81. I. R. Gabdrakhmanov*et al.*, [arXiv:2408.16804 [hep-ph]]; Phys. Atom. Nucl. **87**, no.4, 536-540 (2024)
82. B. A. Magradze, Int. J. Mod. Phys. A **15** (2000), 2715-2734; [arXiv:hep-ph/0010070 [hep-ph]]; R.M. Corless, G.H. Gonnet, D.E.G. Hare, D.J. Jeffrey and D.E. Knuth, Adv. in Comput. Math. **5** (1996) 329.
83. A. P. Bakulev and V. L. Khandramai, Comput. Phys. Commun. **184** (2013) no.1, 183-193; V. Khandramai, J. Phys. Conf. Ser. **523** (2014), 012062 [arXiv:1310.5983 [hep-ph]]
84. K. G. Chetyrkin, Phys. Lett. B **404**, 161-165 (1997)